MODELLING SOIL EROSION IN UN-GAUGED GOLOLE CATCHMENT IN MARSABIT COUNTY, KENYA

GABRIEL NYAGAH NJIRU (BSc. Agricultural Engineering)

A147/OL/22344/2011

A THESIS SUBMITTED IN PARTIAL FULFILMENT OF THE REQUIREMENTS FOR THE AWARD OF THE DEGREE OF MASTERS OF SCIENCE IN LAND AND WATER MANAGEMENT, IN THE DEPARTMENT OF AGRICULTURAL SCIENCE AND TECHNOLOGY OF KENYATTA UNIVERSITY

APRIL 2021

DECLARATION

I (Gabriel Nyagah Njiru) declare that this thesis is my original work and has not been presented for the award of a degree in any other university or any other award.

Gabriel Nyagah Njiru

A147/OL/22344/2011

Signature…………………………………...   Date…………………………...

SUPERVISORS' APPROVAL:

We confirm that the work reported in this thesis was carried out by the candidate under our supervision and has been submitted with our approval as university supervisors.

Dr. Benjamin Danga
Department of Agricultural Science and Technology
Kenyatta University

Signature………………………………….   Date…………………………….

Dr. Kennedy Mwetu
Department of Agricultural and Biosystems Engineering
Kenyatta University

Signature……………………………………   Date…………………………….

Dr. Patrick Kariuki
Department of Geology and Meteorology
South Eastern Kenya University

Signature…………………………………….   Date…………………………….

DEDICATION

Foremost, I dedicate this Thesis to God who has been the source of my strength and inspiration to always move forward. I dedicate this Thesis to my wife Mercy Waithera and children who encouraged me all through until the objective was achieved. I am grateful to them for their prayers and successful wishes prior to all my exams and presentations.

ACKNOWLEDGEMENTS

I express my gratitude to Dr. Benjamin Danga who guided the final steps by offering immense inputs as well as constructive criticism that enabled the successful completion of this thesis. I am sincerely grateful to Dr. Kennedy Mwetu who in a special way contributed his time, expertise and knowledge in tutoring, mentoring and guiding me in the whole process from the conception of the topic, proposal development and overall implementation. He enlisted me in the Remote Sensing Technology Application training jointly facilitated by Regional Centre for Mapping of Resources and Development (RCMRD), Institute of Electrical and Electronic Engineers (IEEE) and Geoscience and Remote Science Society (GRSS) at Kenyatta University where I gained variable knowledge and skills for my research.

I thank in a special way Dr. Patrick Kariuki who was helpful in providing the missing links including data, variable skills in the application of Geographical Information System (GIS) notable was the hands-on use of GIS suit of programs. Indeed, without him it would have been an uphill task to learn the many skills he demonstrated.

I am grateful to Dr. Jayne Mugwe, former Chairperson, Department of Agricultural Resource Management of Kenyatta University who upon request wrote timely recommendation letters to RCMRD (Nairobi) and Kenya meteorological Department (Nairobi) for data acquisition. My sincere gratitude go to all the post graduate seminar attendees for their sincere criticism, variable inputs, insightful comments and encouragement that was most appreciated.

Special thanks go to the RCMRD, Nairobi who acted with speed and provided the requested land satellite (Landsat) images. In the same vein, I sincerely thank the

Kenya Meteorological Department, Nairobi who provided the rainfall data for both Marsabit and Moyale rainfall stations. More so special thanks go to the Kenya Agricultural and Livestock Research Organization (KALRO) Marsabit that was magnanimous in allowing me to use their library that was very useful.

I would like to thank my family: my wife, children, parents' brothers and sisters for their generous spiritual and moral support. I remain grateful to Bishop Peter Kariuki (Marsabit Diocese) for granting me permission and encouragement to study. It is not possible to mention all those who generously assisted me in one way or the other by their names, to all of you I say thanks.

I am also indebted to various authors of books, research journals used for reference.

TABLE OF CONTENTS

LIST OF TABLES

LIST OF FIGURES

LIST OF PLATES

LIST OF ABBREVIATIONS AND ACRONYMS

ASTER	Advanced Spaceborne Thermal Emission and Reflection
a.s.l.,	above sea level
C	Cover
CREAMS	Chemical Runoff and Erosion from Agricultural Management Systems
DEM	Digital Elevation Model
ESRI	Environmental Systems Research Institute
ETM+	Enhanced Thematic Mapper
EUROSEM	European Soil Erosion Model
FAO	Food and Agriculture
GIS	Geographical Information System
GLCF	Global Land Cover Facility
GoK	Government of Kenya
GRSS	Geoscience and Remote Science Society
IDW	Inverse Distance Weighted
IFAD	International Fund for Agricultural Development
IEEE	Institute of Electrical and Electronic Engineers
ILRI	International Livestock Research Institute
ITPS	Intergovernmental Technical Panel on Soils
K	Soil
Km^2	square Kilometre
KALRO	Kenya agricultural and livestock research organization
Km	Kilometre
Landsat	Land Satellite
LISEM	Limberg Soil Erosion Model
LS	Length Slope
M	metres
MS	Mean Square
NSE	Nash-Sutcliffe Efficiency
NDVI	Normalized Difference Vegetation Index
P	Practice
R	Rainfall

R (r)	Pearson correlation factor
R^2 (r^2)	Coefficient of determination
RCMRD	Regional Centre for Mapping of Resources and Development
RS	Remote Sensing
RUSLE	Revised Universal Soil Loss Equation
SDGs	Sustainable Development Goals
SLEMSA	Soil Loss Estimate Model of South Africa
SS	Sum of Squares
SOM	Soil Organic Matter
TGA	Three Gorge Area
T/ha	Tonnes per hectare
T/ha/yr	Tonnes per hectare per year
USGS	United States Geological Survey
USLE	Universal Soil Loss Equation
UTM	Universal Transform Mercator
WEPP	Water Erosion Prediction Project
WFP	World Food Program
WGS	World Geographical System
%	Percentage

ABSTRACT

Soil erosion is a major form of land degradation worldwide with 60% of it attributed to human activities. Golole catchment in Marsabit County with undulating topography is prone to soil erosion and little has been done to avert the soil loss. This study modeled soil erosion between January 2016 and September 2018 for land management in Golole catchment. The Revised Universal Soil Loss Equation (RUSLE) constituting the main agents of soil erosion was modeled in a Geographical Information System (GIS) environment. The objective of this study was to simulate soil erosion for land management in the ungauged Golole catchment using RUSLE. RUSLE input digital data was processed in GIS software using algorithms to yield the catchment's spatial soil erosion loss map. The catchment soil erosion map revealed spatial variation of the rate of soil erosion. The soil loss and risk areas of soil erosion within the catchment were not homogeneous. Golole catchment mean annual soil loss rate was calculated at 279 t/ha/yr that is above the recommended maximum allowable annual soil loss rate of 4 t/ha/yr. The catchment's soil loss rates is described as high and severe representing 70% and 30% of landmass respectively. The model calibration and validation showed strong correlation between the observed and simulated soil losses. The correlation coefficient (r) was 0.97 while the NSE was 95%. The strong correlation is attributable to both observed and simulated input data being either for or from the study area. The model can be adopted in the study area catchment with improvement involving high resolution data covering three parameters: soil, slope length, land cover while rainfall would require more rainfall stations. This study recommends further research in (1) the forest reserve areas that showed the greatest rates of soil erosion menace to determine the underlying causes, and (2) to assess the temporal trends of the soil erosion hazard using high-resolution data.

CHAPTER 1: INTRODUCTION

1.1 Background to the study

Golole catchment located in Marsabit County, Kenya is prone to soil erosion menace that is accelerated by intensive and extensive farming, overgrazing and deforestation. Soil erosion is a worldwide common disaster that leads to the decline of soil fertility, water quality as well as loss of biodiversity (Yang *et al*., 2003). Soil erosion is one of the major threat to land degradation affecting the global production of 95% of food needs of humankind (FAO, 2019). Soil loss deprives people of their livelihood because of physical chemical changes in the soil that reduce crop yield (Toy *et al*., 2002).

Government of Kenya [GoK], (2013) revealed that soil erosion increased the cost of farming forcing farmers to apply extra fertilizers to check on the declining agricultural production. Yang *et al.* (2003) attributed 60% of the global soil loss to anthropogenic activities that in turn led to unsustainable agricultural production. FAO (2019) clarion call was "stop soil erosion to ensure food secure future" emphasize the need to prevent soil erosion.

Globally, food and fibre production including improved nutrition, clean water and air are all dependent on soil (Borrelli *et al*., 2016). According to FAO (2019) soil erosion menace must start being addressed today to prevent more than 90% degradation of earth's soil by the year 2050. Adhikari and Hartemink (2016) noted that soil was a key provider of a myriad of ecosystem services.

FAOSTAT (2005) indicated that 11% of the world's surface comprises of 25% under food production, 25% under grazing, 28% under forest and 36% was the desert. Soil was a limited and irreplaceable resource while its formation is a very slow process hence its loss renders fertile land barren (Ishtiyaq & Verma, 2013). FAO and ITPS (2015) identified soil erosion as the biggest threat to soil. About one third of the land under agriculture globally is affected by soil degradation caused by water and wind (Hurni *et al*., 2008). Despite being the foundation of agriculture, soil continues to receive less attention unlike other resources like vegetation, biodiversity and water (Hurni *et al.*, 2008).

Soil erosion is a threat to food security as it deprives soil of nutrients and water necessary for plant growth (Ganasri & Ramesh, 2015). Dominik *et al.* (2007) and Sanchez (2002) agree that the negative impacts of soil erosion is felt worldwide where 2.6 million people face food insecurity while in East and Sub-Saharan Africa, per capita food production has declined over the last 45 years. The activities that contribute to land degradation are: unsuitable farming methods, poor soil and unsustainable land management practices, deforestation and overgrazing (GoK, 2013). Soil loss is a serious environmental problem that cause land and water degradation due to on-site loss and off-site sedimentation (Tamene, 2014). Anthropogenic activities accelerate soil loss worldwide contributing immensely to land degradation where negative environmental and economic impacts are felt (Prasannakumar, 2011).

Dominik *et al*. (2007) emphasizes that soil erosion remains a key socio economic and ecological problem in Kenya affecting all sectors of the economy; agriculture, hydropower, fisheries and tourism. Kiage *et al.* (2007) linked soil erosion in Kenya to the increased siltation of water bodies (GoK, 2013) pointed out that soil erosion reduced the capacity of soil to filter pollutants and to aid hydrological and nitrogen cycles. Karuku (2018) confirmed that agricultural production in Kenya was greatly undermined by soil erosion. According to Government of Kenya [GOK], (2016), anthropogenic activities like unsustainable land management practices and destruction of vegetation were the greatest threat to land degradation. Kenya's land degradation menace that included soil erosion was severe affecting 61.4% of total land area (GOK, 2016). Kenya's vision 2030 underlines the dire need for sustainable land use (GOK, 2016).

Identifying high-risk areas of soil erosion increases the effectiveness of soil mitigation measures while at the same time reducing soil erosion mitigation cost (Shi *et al*., 2003). The ability to quantify soil loss contributes to effective soil erosion control though the complexity of the variables involved makes prediction of soil loss rate difficult (Prasannakumar *et al*., 2015). Modelling soil erosion aid in quantifying the spatial soil loss and sediment yield as well as identifying soil erosion risk areas for appropriate soil and water management practices (Ganasri & Ramesh, 2015).

The bottleneck associated with erosion modelling was the validation due to the scarcity of data used to compare the models output and the actual soil losses (Ganasri & Ramesh, 2015). This study acknowledges the scarcity of data in the world's developing regions hence employed alternative data sources. Adediji *et al.* (2010) demonstrated the significance of using RS and GIS techniques in soil loss modelling. Adediji *et al.* (2010) confirmed that soil erosion data collection was both expensive and time consuming while the alternative to extrapolate from global data was bound to gross errors and misrepresentation.

FAO and ITPS (2015) points out that soil erosion rates are highly variable both spatially and temporally and therefore, global or regional estimates cannot be translated directly into local rates. This implies that soil erosion mitigation measures will have to be adapted to meet site specific needs both at the farm as well as at catchment levels (FAO & ITPS, 2015).

The ability to quantify soil loss contributes to effective soil erosion control (Ishtiyaq *et al*., 2013). Soil erosion models used to quantify soil loss include and not limited to: the Revised Soil Loss Equation (RUSLE), Soil Loss Estimate Model South of Africa (SLEMSA), European Soil Erosion Model (EUROSEM), Water Erosion Prediction Project (WEPP), Limberg Soil Erosion Model (LISEM) and the Chemical Runoff and Erosion from Agricultural Management Systems (CREAMS).

Physically based models are associated with difficulty and challenges as they demand a lot of data and information. RUSLE was chosen over USLE as it optimized the use of database (Biswas & Pani, 2015).

RUSLE was highly informed by its more than forty years of extensive use, ground truthing and research (FAO, 2019). RUSLE constitutes the main factors causing soil erosion: rainfall erosivity, soil erodibility, slope length, steepness, cover management and support practice (Yahya *et al*., 2013). The choice and use of RUSLE model in this study to quantify soil loss was informed by its all-inclusive representation of the main factors that cause soil erosion (Abdul *et al*., 2015). RUSLE in GIS allows use and analysis of vast amounts of data that would otherwise not be feasible manually (Shi *et al*., 2003).

This study aimed at modeling the spatial rate of soil loss within Golole catchment using remotely sensed digital data in a digital environment as well as ground truthing. The use of digital environment allowed delineation of soil loss severity areas with ease. The digital soil loss map of the catchment can be used by farmers, policy makers and researchers to inform the soil and water conservation measures.

1.2 Statement of the problem

Golole catchment located in Marsabit County, Kenya soil loss has not been quantified. Soil erosion renders the depletion of the limited nutrient rich top soil where farming is possible. The soil erosion menace in the catchment is evidenced by the heavily silted surface water sources comprising of earth pans and dams. Golole catchment is among the many ungauged catchments in Kenya indicating the unavailability of runoff data.

Therefore, this study employed soil erosion modelling techniques, locally available data like rainfall as well as ground truthing. Gunter (2006) recommends the use of rainfall runoff models in ungauged catchments where the rainfall data is used to calibrate the model. Simulation and quantification of soil loss is not well established in Kenya. Therefore, this study contributes in the improvement of soil loss measuring techniques. Effective erosion control measures require the identification of areas vulnerable to soil erosion. This study explored the use of alternative soil erosion quantification technologies using digital data input as well as processing.

Panagos *et al*. (2015) noted that majority of previous studies on soil loss using RUSLE failed to account for the practice factor and attributed it to the lack of soil and water management practices in the respective study areas. This study focuses on soil erosion modelling for management hence takes into account the practice factor that represents part of the management practices that reduce soil erosion like contour ploughing and controlled grazing.

The environmental RUSLE factors represented by R, S and LS remain constant for long period of time e.g. ten years while management factors represented by C, P may change over a short period (Rahman, 2015). Panagos *et al.* (2015) while evaluating the impact of P factor in European Union member target States found that its manipulation where farmers adopted land use management practices (contour farming, stone walls and grass margins) greatly reduced the risk of soil erosion.

1.3 Research objectives

1.3.1 The overall objective

To model soil erosion in ungauged Gololе catchment.

1.3.2 Specific objectives

i. To determine the spatial soil loss in un-gauged Golole catchment in Marsabit county.

ii. To delineate soil erosion prone areas.

1.4 Research Hypotheses

The study tested the following hypotheses:

i. RUSLE simulation does not produce the spatial soil loss within Golole catchment.

ii. RUSLE simulation produces homogeneous soil loss within Golole catchment.

1.5 Significance of the study

Soil erosion assessment is useful for mitigation planning and conservation in a catchment (Hussain & Misra, 2018). Identification of erosion prone areas as well as estimation of the soil loss is essential for selecting appropriate soil and water conservation measures (Pushpalatha *et al.*, 2017). Modelling soil erosion provides quantitative data for soil loss estimation in a catchment (Hussain & Misra, 2018). Effective soil erosion control requires prediction of the amount of soil loss (Ishtiyaq

& Verma, 2013). Shi *et al*., (2003) demonstrated the necessity for soil conservation in the Three Gorge Area (TGA) in China for ecological sustainability as well as the proper functionality of the Three Gorge Dam reservoir. Pushpalatha (2017) found that areas having lower normalized difference vegetation index (NDVI) resulted in higher values of C factor.

RUSLE layers in GIS can be adjusted to evaluate their corresponding effects on different land cover and land use scenarios aimed at mitigating soil erosion (Hudson, 2005). Carlos (2010) demonstrated the ability of the RUSLE model adjustment in GIS environment to build up different scenarios of vegetative cover for mitigation against soil loss. The NDVI monitors vegetation spatial and temporal healthiness (Carvalho *et al.,* 2014). The acceptance and adoption of soil mitigation measures by users in order to improve productivity is largely influenced by their demonstrability (Tamene, 2014). Land managers and policy makers are interested in both soil loss and its spatial distribution within the catchment for successful soil erosion management (Phinzi & Ngetar, 2017).

1.6 Justification of the study

The ungauged Gololе catchment is prone to accelerated erosion that threatens the current and future sustainable ecosystem services like food. The magnitude and consequences of soil erosion menace in Gololе catchment is not clearly known and documented. Therefore, Gololе catchment soil erosion menace receives little or no attention from farmers and decision makers. There is need to address this gap of quantifying soil loss in order to inform the choice of soil loss mitigation measures as well as the policy. This study creates soil erosion awareness among farmers and decision makers.

The major competing land uses in Golole catchment include farming, wildlife, grazing and physical infrastructure that are also the major causes of soil erosion. The quantified soil erosion will inform the soil and water conservation measures relevant to the targeted locality or catchment.

The digital soil loss map of the catchment can be used as a demonstration tool by agricultural extension officers to pinpoint areas prone to severe soil erosion as well as inform policy on sustainable agriculture. The soil erosion map directly helps farmers in planning and making investment decisions on soil and water conservation measures.

1.7 The scope of the study

This study modelled Golole catchment's soil erosion for land management using digital techniques in a GIS environment. The study conducted ground truthing to validate the soil erosion model output through insitu observation and analysis of the soils, land use and land cover. The rainfall data was used to calibrate the model. The spatial distribution of soil loss within the catchment was analyzed in order to delineate the erosion risk areas.

1.8 Conceptual framework

The RUSLE five factors remained the model input as well as the main drivers of soil loss in Golole catchment. The magnitude of soil loss was predominantly determined by erosivity and erodibility (Angima *et al*., 2003). Erosivity is associated with the rainfall, being a measure of forces applied to the soil causing soil detachment and transportation while erodibility is dependent on soil physical chemical characteristics, being a measure of susceptibility of soil to erode. On the other hand, soil erosion is highly dependent on land gradient while anthropogenic activities aggravate soil erosion through the alteration of land cover and use (Yang *et al*., 2003).

Modelling soil erosion in Golole catchment envisioned data input, analysis and output in a GIS environment (Figure 1). The GIS environment implied that all the input data has to be in digital format. The digital data representing each of the five RUSLE factors was processed independently using the respective algorithms in a GIS environment. The final overly operation was executed to combine the five RUSLE layers and derive the erosion risk map of the catchment.

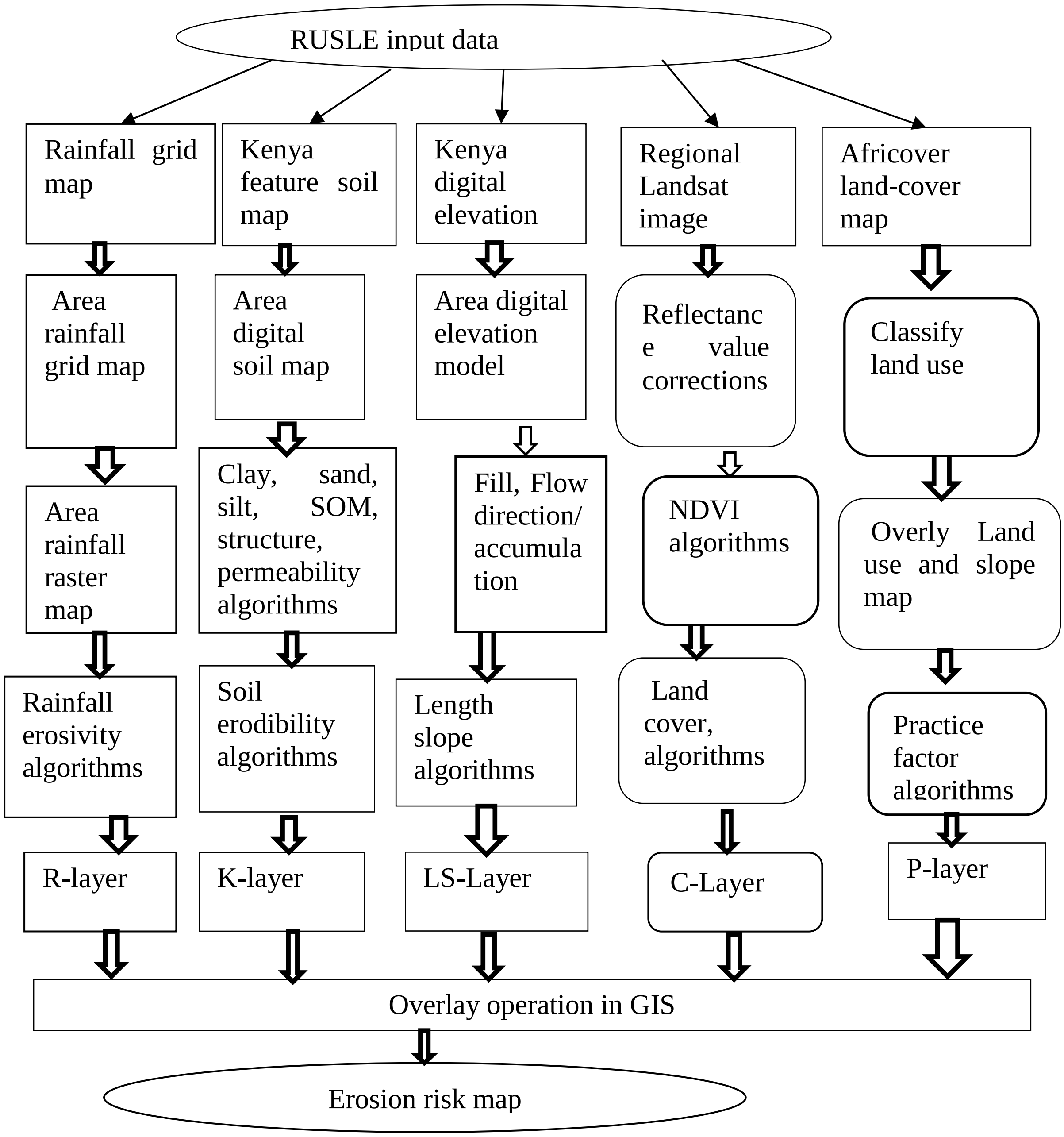

Figure 1.1 Conceptual framework

CHAPTER 2: LITERATURE REVIEW

2.1 Overview of soil erosion

Soil erosion and degradation of land resources are highly significant spatio-temporal phenomena in many countries (Fistikoglu & Harmancioglu, 2002). The drivers of accelerated soil erosion include rapid population growth that adds pressure on land leading to cultivation on steep slopes, clearing of vegetation and overgrazing (Abate, 2011). Soil erosion threatens the global food security as well as the achievement of the Sustainable Development Goals (SDGs) as it hinders growth of nutritious food, contribute to ill-being of ecosystems, affects water supplies, damages infrastructure, contributes to migration and exacerbates climate change (FAO, 2019)

According to FAO, IFAD and WFP (2015) a worrisome tread was noted where an estimated 23.2% of people living in the Sub-Saharan Africa were undernourished. About 795 million people globally faced hunger out of which 780 million people lived in the developing countries (FAO, IFAD & WFP, 2015). Jeff (2003) attributed Kenya’s food shortage to soil erosion menace that deprived soil of its vital nutrients, water and biodiversity necessary for plants growth. In order to enhance sustainable agricultural production, soil and water conservation will have to be part and parcel of land management at household and community levels (Hurni *et al.*, 2008).

Bewket and Teferi (2009) on conservation planning agreed that severe erosion prone areas could be delineated and prioritized for erosion mitigation. Soil erosion is one of the major drivers of land degradation globally with both on-site and off-site negative effects (Abate, 2011). The on-site and off-site impact of soil erosion is soil loss and siltation / pollution of water bodies like water reservoirs, rivers and lakes. Carlos *et al*. (2010) emphasized on the need for quantitative estimates of soil erosion by water to inform land use management, soil and water conservation that leads to sustainable agricultural production while supporting forestry and biodiversity.

2.2 Soil loss models

The existing soil loss quantification models can be broadly categorized into physical, conceptual and empirical models. Physical models are physical copies of an object that may be the same, smaller or larger. Conceptual models are based on mental concepts, imaginary or ideas. Empirical models are created by observation or experiment.

2.2.1 Physical based models

Physical based modelling involves creation of real world representations of events like soil erosion capable of simulating their physical characteristics. The following is a discussion of some of the widely used physical models.

The EUROSEM model was developed by European scientist for use in European Community countries. The model is based on a single event that requires daily input of soil water balance data applied in small catchments. The model inputs include topography, soil, vegetation and rainfall while its output are total runoff, total soil loss, the storm hydrograph and storm sediment graph (Obeta & Adewumi, 2013). The EUROSEM model requires a large amount of input data hence was not prioritized for use in this study. For example, rainfall alone would be required in depth, intensity, volume and cumulative (Morgan *et al.*, 1998). Tamene (2014) underlined the minimal operational tools that supported soil loss measures in data scarce regions of the world including the developing countries for example the unavailability of rainfall intensity data.

The LISEM is a hydrological model developed in the Netherlands in 1996. The model simulates runoff, sediment and erosion. This model factors include rainfall, vegetation, soil and topography (Torsten & Jannes, 2014). This model is based on EUROSEM (Morgan *et al*., 1998) and involves very many parameters like rainfall interception, surface storage in micro depressions infiltration, vertical water movement through the soil and overland flow among others. This model was not used in this study due to its complexity and large data input requirement with some data not easily obtainable.

The WEPP model was developed by the USDA. It models soil loss by adding the sediment loss from the inter-rill areas to the rill erosion. The model is also based on a continuous simulation approach requiring daily calculations of soil water balance (Obeta & Adewumi, 2013). The use of this model in this study was not feasible as the model is highly complex and requires large amount of input data (Morgan, 1988). The increased data requirement of a model will improve the quality of the model but also be expensive (Morgan *et al*., 1998).

The CREAMS soil erosion model developed by USDA consists of three major components: hydrology, erosion/sediment and chemistry. The hydrology simulation involves rate of runoff, evapotranspiration, soil moisture and percolation while the chemistry simulation involves fertilizers and pesticides movement and forecast single rainfall event. CREAMS soil erosion model assumes a homogeneous soil, land use and precipitation occurrences (Joy & Muthukrishna, 2017). CREAM erosion prediction applies complex set of equations and logic besides the large number of parameters (Silburn & Lock, 1989). This model was therefore not considered due to its complexity.

2.2.2 Empirical models

Empirical based modelling involves the creation of real world representations of events like soil erosion based on observation and experiment. The most widely applied empirical models are the Soil Loss Estimation Model for Southern Africa (SLEMSA), Universal Soil Loss Equation (USLE) and Revised Universal Soil Loss Equation.

SLEMSA model was applied in South African countries. This model is based on sub-models each suited to a particular erosion parameter like soil, climate and land use (Smith, 1999). According to Smith (1999) SLEMSA model can differentiate areas of high and low erosion potential. Researchers had begun the journey of quantifying soil erosion about half a century ago by assessing the major variables that contributed to soil erosion by water (Wischmeier & Smith, 1978).

Wischmeier and Smith (1978) developed the Universal Soil Loss Equation (USLE) using historical data on major variables that affected soil erosion by water. The USLE was originally developed for soil erosion estimation for conservation planning in croplands with gentle slope (Wischmeier & Smith, 1978). The erosion control practices were tailored to the needs of specific farms where USLE relied on finding its parameters in already printed tables and charts (Renard *et al*., 2010).

The USLE development was to be unlimited geographically hence the use of the word "Universal" (Wischmeier & Smith, 1978). However, this was not the case since USLE application was only limited to croplands and areas with gentle slope (Foster, 2003). USLE factors were realized in a unit plot that presented the worst management case scenario measuring 22.1 m long with a slope of 9% in a continuous tilled fallow and up and down hill tillage (Renard *et al*., 2010).

The plot was the basis upon which all other parameters: topographical, cover, management, conservation practices were compared (Renard *et al*., 2010). The USLE, a precursor to RUSLE was revised due to its apparent limitations in order to incorporate advanced knowledge in soil erosion, evolving technology and more accurately estimate soil loss from both cropped, disturbed, rangeland areas and hillslopes (Renard *et al*., 2010). The USLE and RUSLE empirical erosion models were widely used in USA and other countries (Renard *et al*., 2010).

The revision of USLE to RUSLE 1 widened its applications to different situations including forests, rangelands, and disturbed areas (Renard *et al*., 1997). While USLE is an index empirically based model, both RUSLE 1 and RUSLE 2 combine both index and process (Foster, 2003). RUSLE 2 is superior to RUSLE 1 as it can analyze soil erosion in very complex hillslopes (Foster, 2003).

RUSLE maintained the basic structure of USLE but the algorithms used to calculate individual factors changed significantly including computerization (Renard *et al*., 1995). According to Smith (1999) RUSLE was flexible hence the user was responsible for manipulating the data sets. RUSLE improvements over USLE involved: more data to cover different scenarios like cropping, forest and rangelands, incorporated a process based approach where algorithms were adopted that gave its flexibility (Smith, 1999). The USLE factors underwent significant changes in moving to RUSLE as explained below:

The R factor is determined by the product of energy and the maximum 30 minutes rainfall intensity of each storm. Changes to R-factor included reduction of R values in areas of flat slopes with intense storms as the ponded water reduced erosivity (Renard *et al*., 2010). The second change involved modification of R factor following high erosivity in frozen and thawing soils that experienced weakened soil structure (Renard *et al*., 2010). The K factor (erodibility) is a measure of effects of soil properties and soil profile on soil erosion. USLE was limited to soil inherent properties implying that the soil properties are determined under unit plot conditions (Renard *et al*., 2010).

This was cumbersome taking not less than two years. In USA RUSLE 1 K values were site specific obtained from USDA databases while in other countries users resorted to soil sampling coupled with soil erodibility normograph (Renard *et al*., 2010).

The LS factor sensitivity to both slope length and steepness was considered with more attention geared towards obtaining good estimates of slope steepness. USLE used quadratic relationship with slope steepness while RUSLE adopted a linear relationship in addition to computer program that accommodated complex slopes (Renard *et al*., 2010).

Both C and P factors represents conditions that can be managed to reduce soil erosion. The C and P factors in USLE were a measure of how erosion from the current condition compared with that of Unit Plot conditions (considered the worst case scenario) (Renard *et al*., 2010). RUSLE adopted a sub-factor approach that computed the C and P factors as a function of sub-factors (Renard *et al*., 2010). The C factor reflects the positive impacts of management emanating from such factors like vegetation, soil biomass and roughness while the P factor reflect the positive impacts of management emanating from practices that control (change direction and speed) of runoff: strip cropping, terraces, contour tillage and subsurface drainage (Renard *et al*., 2010).

The C factor five multiplicative sub-factors: prior land use, crop canopy, surface cover, surface roughness and soil moisture (Renard *et al*., 2010). RUSLE adopted a sub-factor approach that computed the C factor as a function of five sub-multiplicative factors: prior land use, crop canopy, surface cover, surface roughness and soil moisture (Renard *et al*., 2010). The RUSLE C sub-factor approach was economical as opposed to the expensive USLE that was dependent on specific land use requiring different datasets for each possible land use (Renard *et al*., 2010).

The P factor separate multiplicative sub-factors in RUSLE include contouring, strips, terraces and subsurface drainage (Renard *et al*., 2010). The RUSLE effect of contouring was extensively evaluated including a broader array of strip cropping and terracing than in USLE (Renard *et al*., 1995).

2.3 Determination of soil loss using RUSLE

2.3.1 RUSLE model selection

Empirical models could be used as qualitative screening tools to identify areas prone to erosion (Smith, 1999). A theoretical evaluation and sensitivity ananlysis of SLEMSA, USLE and RUSLE, Smith (1999) found that RUSLE was more flexible and dynamic as opposed to the strict empirical structures of ULSE and SLEMSA. More so RUSLE model response was rational hence its soil loss patterns were acceptable while SLEMSA model was very sensitive to changes in rainfall and slope (Smith, 1999).

RUSLE equation predicts annual soil loss resulting from rill and sheet erosion (Hussain & Misra, 2018; Prasannakumar, 2011). RUSLE model can predict the spatial pattern of soil loss over a large region (Rahaman, 2015). According to Birham (2016), RUSLE was the most widely used soil erosion model to estimate soil loss because of its simplicity, limited data requirements and compatibility with GIS. RUSLE inputs parameters can be derived from existing databases and digital data like satellite images (Ganasri & Ramesh, 2015). The RUSLE factors are location specific hence can be calibrated for a specific area to predict the rate of soil loss (Fistikoglu & Harmancioglu, 2002).

According to Prasannakumar (2011) and Angima (2003) RUSLE is also appropriate in assessing the spatial distribution of soil erosion and predicts erosion rate of an ungauged catchment. GIS has enabled RUSLE parameters to be spatially represented (Abate, 2011).

RUSLE is applied worldwide to predict soil loss because of its convenience and compatibility with GIS (Carlos, 2010) and can be used to simulate anthropogenic impacts on the environment (Hudson, 2005).

In developing countries availability of soil erosion data sets is scarce or requires ample time, money and effort to prepare (Hussain & Misra, 2018). Abate (2011) and Hurni (1985) demonstrated the use of different empirical equations used to estimate rainfall values in data scarce countries and remote regions. In this research RUSLE was adopted due to its flexible and dynamic empirical structure, less data input parameters and its widespread use in many countries in the world.

2.3.2 RUSLE application and impact

RUSLE can be integrated effectively with Remote Sensing (RS) and GIS technologies in modeling soil erosion (Hussain, 2010). Carlo *et al*. (2010) demonstrated that the estimation of soil loss using RUSLE in a GIS framework in Central Chile allowed speedy evaluation of diverse scenarios that informed water and soil conservation measures.

Carvalho *et al*. (2014) demonstrated use of NDVI time series obtained from satellite images to determine RUSLE cover factor in tropical areas. This study employed remote sensed data in a GIS environment to derive the C and P factors. The availability of spatial digital data has made it possible to study the possibility of using algorithms in a GIS environment for enhanced accurate soil loss results.

2.4 Delineation of risk areas of soil erosion using RUSLE

According to Phinzi and Ngetar (2017) the major drawback of soil erosion research is limited information on where soil loss was highly concentrated. RUSLE model was used to perform sensitivity assessment where different soil erosion parameters were chosen and adjusted (Tamene, 2014). Ashiagbor *et al*. (2013) modelled RUSLE in a GIS environment and categorized the Densu River Basin soil erosion risk areas as: 88% low, 6% moderate, 3% high and 3% severe. Moses (2017) generated a soil erosion map of River Nzoia Basin, Kenya using RUSLE in a GIS environment and linked the high erosion risk areas to cropland, deforested and hilly areas. Kumar *et al*. (2014) integrated RUSLE, RS and GIS in generating soil erosion map of the Kangra region of Western Himalaya, India and observed that the undulating terrain was the main cause of soil loss. This study determined the risky areas of soil erosion using RUSLE in a GIS environment.

CHAPTER 3: MATERIALS AND METHODS

3.1 Study area

The study area is located on the Eastern slopes of Mt. Marsabit in the central region of Marsabit County, Kenya (Figure 3.1). According to Marsabit County integrated development plan (2013 - 2017), administratively the county comprises of four Sub-Counties: Saku, Laisamis, North Horr and Moyale covering an area of 70,961.2 km^2. According to 2009 Kenya National Population and Housing Census, the county had a projected population of 316,206 people in 2012 and 343,399 in 2015. Mt. Marsabit lying about 1500 m above mean sea level is centrally located in Saku Sub-County.

The study area exhibits undulating terrain with isolated steep slopes and hills occupying an area of 1,886 km^2 lying between latitude 02^o 0^o and $02^o24^o47^o$ North and longitude 37^o 53^o17^o and $38^o28^o8°$ East (Figure 3.2). The area stretches 67 km with the widest section measuring 35 km. According to Kenya ecological zones (Appendix I, Table A1), the study area ecologically varies from semi-humid to semi-arid with a mean annual rainfall of 875 mm. The study area soils can be described as well drained, moderately deep, dark reddish, brown to dark red friable clay textured.

According to Food Agricultural Organization (FAO) soil classification, the study area soils vary geographically comprising of lithosols, chromic cambisols, pellic vertisols, Eutric nitosols, mollic andosols, calcic xerosols/yermosols and calcic fluvisols (Appendix VI, Table A2). The study area land cover includes woody trees, low shrubs and herbaceous plants. The area boasts of herbaceous crops and a dendritic drainage pattern of ephemeral rivers.

Figure 3.1: **Map showing the study area in Marsabit County, Kenya**

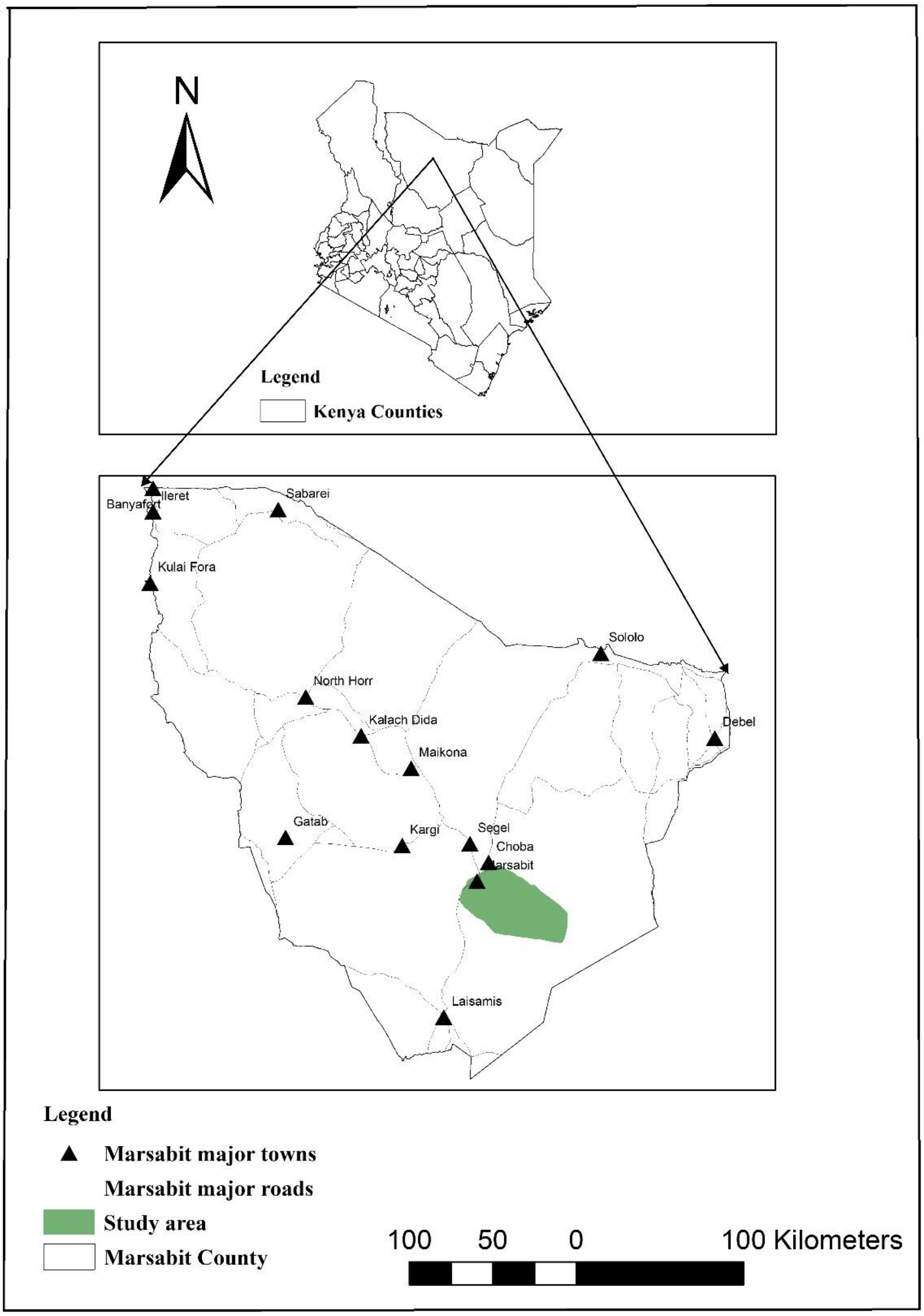

3.2 RUSLE factors' algorithms

Table 3.1: RUSLE factors algorithms

Factor	Algorithms
R factor	$R = -8.12 + (0.56\ xP)$ -------------1 R is the rainfall factor and P is the mean annual rainfall (Hurni, 1985).
K factor	$K = 27.66m^{1.14}x\ 10^{-8}x(12 - a) + 0.0043x(b - 2) + 0.0033x(c - 3)$------------------------2 K= Soil erodability factor (ton·hr−1·ha−1·MJ·mm), m = (Silt % + Sand %) × (100 – clay %), a = % organic matter, b = structure code: 1) very structured or particulate, 2) fairly structured, 3) slightly structured, and 4) solid, c = profile Permeability code: 1) rapid, 2) moderate to rapid, 3) moderate, 4) moderate to slow, 5) slow, 6) very slow (Wischmeier and Smith, 1978). Equation used to derive soil organic matter: $SOM = 1.72\ x\ OC$-------------------------3 SOM is the soil organic matter and OC is the soil percentage organic carbon content (Baldock and Nelson, 2000).
LS factor	$LS = ([Flow\ accu - mulation]x[cellsize]/22.1)^{0.4}x[\sin(localslope\ (degrees))x0.0896/0.0896]^{1.3}$--4

LS is the length slope factor; flow accumulation is the number of cells contributing to flow into a given cell. Cell size is the ground resolution of 30 meters (Moore and Burch, 1986a, 1986b).

C factor

Equation used to calculate Landsat image reflectance value:

$\rho\lambda = M\rho Qcal + A\rho$ --------------------------------5

Where ρλ is the TOA planetary reflectance, Mρ is band multiplicative rescaling factor, Qcal is quantized and calibrated standard product pixel values (DN) and Aρ is the band specific additive rescaling factor.

Equation used to correct reflectance for the sun angle:

$\rho\lambda = \rho\lambda / Cos\Phi SZ = \rho\lambda / Sin\Phi SE$ -----------------6

Where ρλ is the Top of Atmosphere (TOA) planetary reflectance, ΦSE is the local sun elevation angle (Sun Elevation), ΦSZ is the local solar zenith angle ($\Phi SZ = 90^0 - \Phi SE$).

Equation used to calculate the NDVI.

$NDVI = \frac{(Band\ 5 - Band\ 4)}{(Band\ 5 + Band\ 4)}$----------------------------7

Where band 4 is the red band while band 5 is the infra-red band.

Equation used to estimate the land cover factor

$C_{r=}\left[\left(-NDVI+\frac{1}{2}\right)\right]$--8

	Where C_r is the land cover factor (University of Toronto Admin 2015; Durigon, 2014).
P factor	This was derived in ArcMap 10 using reclassified percentage slope map and practice map (agriculture and non-agriculture) of the study area.
Soil loss (A)	The five RUSLE factors were overlaid to derive the soil loss $A = RxKxLSxCxP$-----------------------------------9 Where A is the soil loss, R is the rainfall, K is the soil, LS is the slope length, C is the crop and P is the practice factors.

3.3 Geographical information system software

In this study RUSLE algorithms shown in table 3.1 were used to derive the five RUSLE thematic layers (factors) in a GIS environment. All maps were projected using Universal Transform Mercator (UTM) Zone 37N using the World Geographical System (WGS) 1984 datum corresponding to standards used by Survey of Kenya. GIS ArcMap 10 software that was designed by the Environmental Systems Research Institute (ESRI) was used to model RUSLE using a wide range of analytical and geo-processing tools.

The Marsabit county shape file map was derived from Kenya counties' shape file map in ArcMap 10. The Marsabit County was selected and exported as a new shape file. The Marsabit county shape file was used to derive the Marsabit county land cover map through the clipping process in ArcMap 10. The study area polygon map was drawn using editor tool bar guided by Marsabit county landcover as base map. The five RUSLE factors were processed in ArcMap 10 as follows:

3.3.1. Rainfall factor

The ArcMap 10 spatial analyst hydrology, interpolation and map algebra calculator tools were used to derive the various spatial rainfall maps. Inverse Distance Weighted (IDW) tool was used to derive the rainfall raster map using rainfall data. The study area map was used to extract the rainfall raster map of the study area using analysis extract by mask tool in ArcMap 10. The math algebra tool in ArcMap 10 was executed to output the R-factor map of the study area using Hurni's equation 1 shown in table 3.1.

3.3.2. Soil factor

The study area soil map was clipped from the Kenya digital soil map. The three raster maps of silt, sand and clay were derived in ArcMap 10 using conversion tools. The polygon to raster tool was executed to output the silt, sand and clay raster maps after entering the soil map of the study area as input feature and using the respective percentage textural class in the attribute table as value field. The soil organic matter (SOM) was derived using equation 3 shown in table 3.1. In ArcMap 10, a field for SOM in the study area soil map attribute table was added. The conversion polygon to raster tool was executed to output SOM map with input feature being the soil map of the study area while the value field being SOM. The soil structure was derived by adding a field in the soil map of the study area attribute table representing the structure code. The conversion polygon to raster tool was executed to output the structural code map with the soil map of the study area as input feature and structural code as value field.

A similar process was followed as above to derive the permeability code. A field was added in the soil map of the study area attribute table to represent the permeability code. The polygon to raster tool was executed to output permeability code map after entering soil map of the study area as input feature and permeability field code in the value field. Finally, the six soil raster maps comprising of the clay, sand, silt, organic matter, structure code and permeability code were entered as map algebra expressions according to equation 2 shown in table 3.1 using spatial analyst math algebra raster calculator tool to output the soil factor map of the study area.

3.3.3. Slope length factor

The digital elevation model (DEM) of the study area was extracted from the Kenya DEM with a cell size (ground resolution) of 30 m. The analysis extract by mask tool was executed to output the DEM of the study area after entering the Kenya DEM as raster input and study area map as feature extract mask. To derive the flow accumulation map, ArcMap 10 hydrology tools were used to perform sequentially fill and flow direction processes.

To execute these processes, ArcMap 10 hydrology tools: fill, flow direction and flow accumulation were lodged sequentially. First, the fill tool was executed (to fill sinks) to output the surface raster map of the study area with the input surface raster being the DEM of the study area.

Secondly, the flow direction tool was executed to output flow direction raster map with surface raster map (after fill) as input surface raster. Thirdly, the flow accumulation tool was executed to output the flow accumulation raster map with flow direction map as input raster. The DEM of the study area was also used to derive the local slope gradient map in ArcMap 10 spatial analyst surface tools. The slope tool was executed to output the slope raster map in degrees with the DEM of the study area as input raster. Finally, equation 4 shown in table 3.1 was executed in ArcMap 10 math algebra raster calculator with the flow accumulation and local gradient maps entered as map algebra expressions to output the LS factor map of the study area.

3.3.4. Land cover factor (C)

The Normalized Difference Vegetation Index (NDVI) map was derived using band 5 and 4 of the landsat 7 and 8 images in ArcMap 10 using equations 5, 6 and 7 shown in table 3.1. The satellite images of the study area were extracted by mask tool from the NDVI images in ArcMap 10. The correlation between C and NDVI was determined in ArcMap 10 spatial analyst map algebra raster calculator using equation 8 (Table 3.1).

3.3.5. Practice factor

To derive the slope of the study area in percentage, the data management projections and transformations, project raster tool was executed to transform the DEM of the study area from geographical coordinate to projected coordinate system. Secondly, spatial analyst surface slope tool was executed to output slope map of the study area in percentage with the project DEM (degree) of the study area as input raster.

The percentage slope raster map was reclassified into six classes by converted it into a polygon map using the raster to polygon tool. In the attribute dialogue box, the reclassified polygons were merged using the attribute table, grid code, and unique values. The merging was completed by repeating the process for all unique values from 1 to 6. The analysis overly union tool was executed to combine the percentage slope and practice maps of the study area. A field representing practice factor values was added in the attribute table based on the slope and practice type. Finally, the added practice field in the attribute table was used to derive the practice factor map using conversion polygon to raster tool.

3.4 RUSLE model calibration and validation.

The model was calibrated and validated using statistical tools in an Agricultural and Meteorological Software. The degree of collinearity between the simulated and observed data was established using Pearson's correlation coefficient (r), coefficient of determination (R^2) and Nash-Sutcliffe efficiency (NSE).

The correlation coefficient is a statistical measure of the strength of the relationship between two variables with a range between -1.0 and 1.0. A correlation of -1.0 or 1 shows a perfect correlation that is negative and positive respectively. A correlation of zero (0) indicates no relationship between the two variables. Pearson's correlation coefficient is R but R^2 is squared of Pearson's correlation coefficient (Agricultural and meteorological software, 2019). Nash-Sutcliffe efficiency indicates how well the plot of observed versus simulated data fits the 1:1 line. With NSE = 1 corresponding to a perfect match of the model to the observed data while NSE = 0, indicates that the model predictions are as accurate as the mean of the observed data and NSE < 0, indicates that the observed mean is a better predictor than the model (Agricultural and meteorological software, 2019).

3.4.1 Rainfall factor

The rainfall factor was derived from the data collected from two meteorological stations located in Marsabit county headquarters that falls within the study area and the meteorological station located in Moyale were used to calibrate the model (Appendix VII). The Moyale meteorological station is located outside the study area but was adopted since it has similar geographical characteristics as the target catchment's lowland. The Inverse Distance Weighted (IDW) interpolation method in ArcMap 10 was used to generate both rainfall raster maps and rainfall factor maps.

The rainfall data between the years 1980 to 2010 was used to calibrate the model while between 2011 and 2013 was used to validate the model. The Kenya rainfall grid sourced from International Livestock Research Institute (ILRI, 1998), figure 3.2 was used to further calibrate the model.

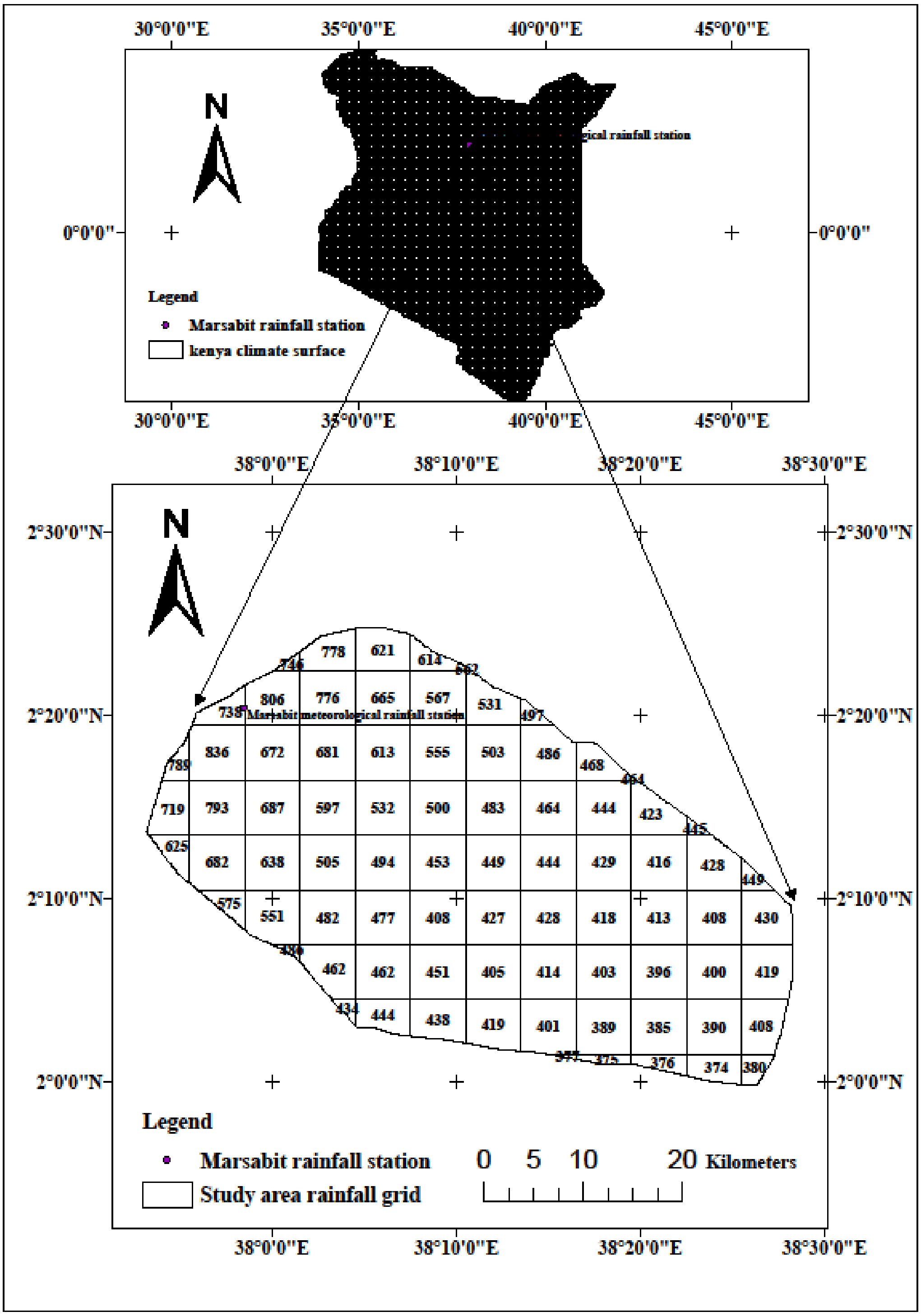

Figure 3.2. *Rainfall grid of Kenya and study area*

3.4.2. The soil factor

The revised digital soil map of Kenya sourced from Regional Centre for Mapping of Resources and Development (RCMRD) Nairobi, Kenya (2016) was used to derive the K-factor maps. The K-factor was derived using the soil factor equations 2 and 3 shown in the RUSLE factors' algorithms (Table 3.1), (Wischmeier and Smith 1978; Renard et al., 1995). Silt, sand and clay parameters were directly derived from the digital soil map.

The soil organic matter parameter was indirectly derived from the digital soil map (Baldock and Nelson, 2000). The soil structure and profile permeability parameters were categorized under three structural codes (2, 3 and 4) and (2, 3 and 5) respectively (Wischmeier and Smith, 1978; Renard *et al*., 1995). The K factor was based on a scale from 0 to 1, where 0 refers to soils with least susceptibility to erosion and 1 to soils which are highly susceptible to erosion by water.

3.4.3 The length slope factor

The DEM with a ground resolution of 30 m sourced from the United States Geological Survey (USGS) (2016) was derived from the Advanced Spaceborne Thermal Emission and Reflection (ASTER). The LS-factor parameter maps: DEM sink filled, flow direction, flow accumulation and slope gradient maps were derived independently using the equation 4 shown in the RUSLE factors algorithms (Table 3.1), (Moore and Burch, 1986a, 1986b).

3.4.4 The cover factor

The C-factor is a relation between erosion on bare soil and a land cover type and density, adopting a value of 1 for bare soils and less than one for more reducing erosion land cover. The NDVI maps were derived from Landsat images sourced from the Regional Centre for Mapping of Resources and Development (RCMRD) Nairobi, Kenya (2016). The Landsat images were acquired from Landsat Enhanced Thematic Mapper (ETM+) imagery from Global Land Cover Facility (GLCF). The Landsat images were processed for reflectance value, reflectance correction and NDVI using equations 5, 6, and 7 shown in the RUSLE factors' algorithms table 3.1. The land cover factor was derived using equation 8 shown in the RUSLE factors' algorithms table 3.1(University of Toronto, Admin 2015; Carvalho, 2014).

The study area Landsat images of March for the years between 2009 and 2017 acquired from Landsat Enhanced Thematic Mapper (ETM+) imagery from Global Land Cover Facility (GLCF) were used to derive the land cover factors for calibration and validation. The month of March was chosen as the period when vegetation is highly stressed from soil moisture hence the land is vulnerable to soil erosion.

3.4.5 The modified P factor

The practice factor values range from 0 to 1 with the lower values indicating better practice for controlling soil erosion. The percentage slope and major land use concept was adopted in this study.

The practice factor was influenced by slope and two categories of landuse that is agriculture and non-agricultural (Wischmeier and Smith, 1978). The Africover land-cover maps of 2010 to 2014 produced from the Landsat ETM+ images sourced from the Regional Centre for Mapping of Resources and Development (RCMRD) Nairobi, Kenya (2016) were used to derive the major land uses in the study area. The slope categories were derived from the DEM of the study area.

The two major land uses (agricultural and non-agricultural) and the DEM percentage polygon maps were overlaid in GIS to produce the study area map with the two major land uses flagged by their respective percentage slope as shown in the conservation practice factors' table 3.2. The agricultural lands were classified into six slope categories and assigned p-values respectively while all non-agricultural lands were assigned a P value of 1 as shown in the conservation practice factors table 3.2.

Table 3.1. Conservation practice factors, Wischmeier and Smith (1978)

Land use	Percentage slope	P-factor
	0.00 – 5.00	0.10
	5.00 – 10.00	0.12
	10.00 – 20.00	0.14
Agriculture	20.00 -30.00	0.19
	30.00 – 50.00	0.25
	50.00 – 100.00	0.33
Other land	All	1.00

3.4.6 The soil loss (A)

The five RUSLE thematic layers were overlaid to derive the soil erosion map using RUSLE equation shown in the RUSLE factors algorithms (Table 3.1).

3.5 Ground truthing

A transect route across the catchment's agricultural area was used to collect insitu information on soil and vegetation to verify the soils, land cover and land use. In addition observation was made on the soil, slope, water, vegetation, food crops, cash crops as well as soil and water conservation measures. The Global Position Satellite (GPS) points shown in figure 3.3 were used to verify the soil, topography, and landcover and landuse type.

Figure 0.3. **Map showing transect route**

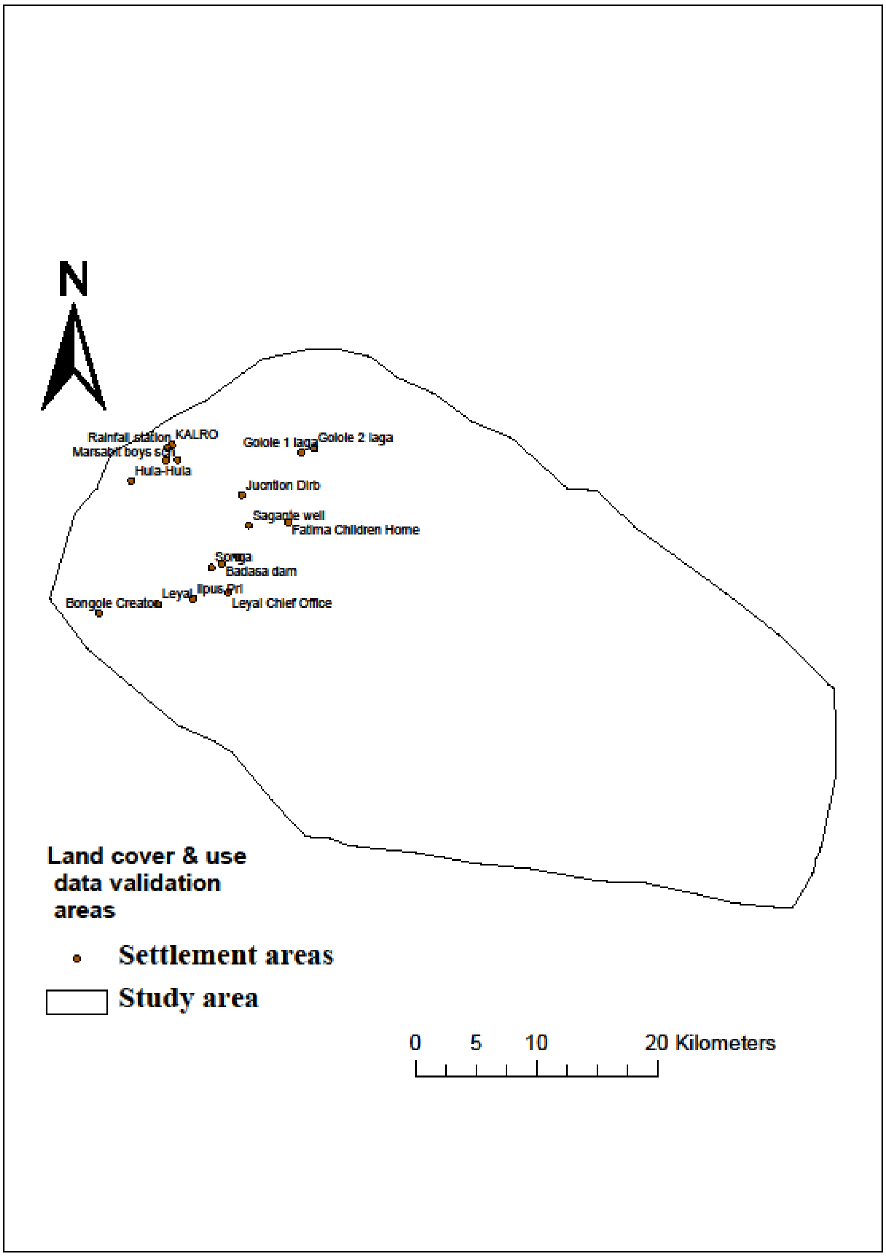

3.6 Hypotheses testing

Hypothesis 1

$$H_{0:}\ \mu = 0$$

$$H_a\!: \mu \neq 0$$

Hypothesis 2

$$H_{0:}\, \sigma = 0$$

$$H_a : \sigma \neq 0$$

3.7 Delineation of risky areas of soil erosion

The soil loss homogeneousness within the catchment was observed in order to delineate the risky areas of soil loss. The study adopted appropriate soil loss severity classes for the different soil losses.

CHAPTER 4: RESULTS

This chapter presents the results following the execution of the steps outlined in the methodology discussed in chapter three.

4.1 RUSLE Model calibration and validation

4.1.1 Rainfall factor

The spatial interpolation inverse distance weighted (IDW) tool was used to generate rainfall maps of the study area. An example of study area rainfall raster map (Figure 4.1) and rainfall factor map (Figure 4.2) is shown below.

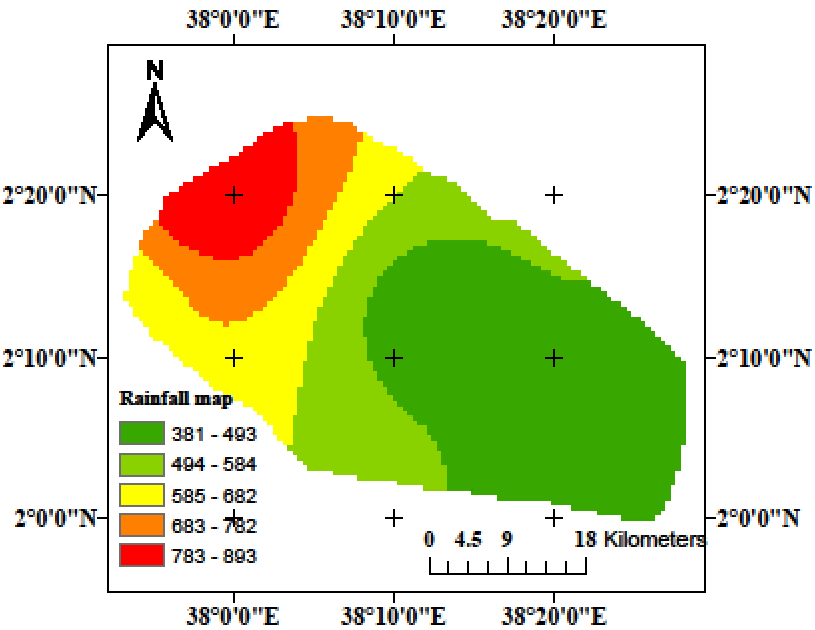

Figure 0.1. Rainfall data map

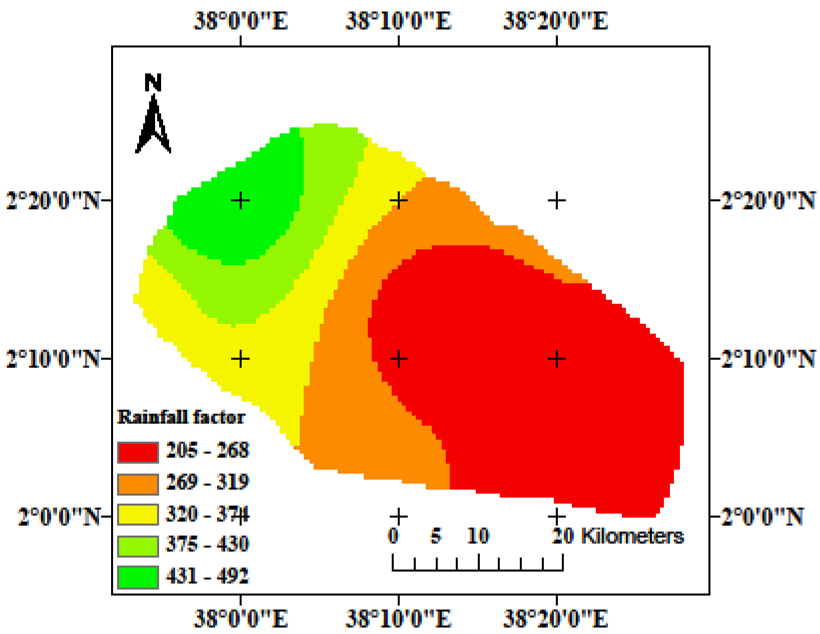

Figure 0.2. Rainfall data factor map

4.1.2 Soil factor

The study area soil was observed as predominantly clay to loam similar to the derived soil maps of the study area.

4.1.3 Length slope factor

The length slope factor was derived using the DEM of the study area.

4.1.4 Land cover and practice factor

In the cultivated areas contour farming was observed while other conservation measures were missing. The rangeland lands had vegetation depleted to minimal vegetation and bare land due to overgrazing.

The cover factor maps were derived from Landsat image sourced from RCMRD Nairobi, Kenya (2016). An image acquired on 15th March 2017 was used to derive the land cover factor map shown in figure 4.3.

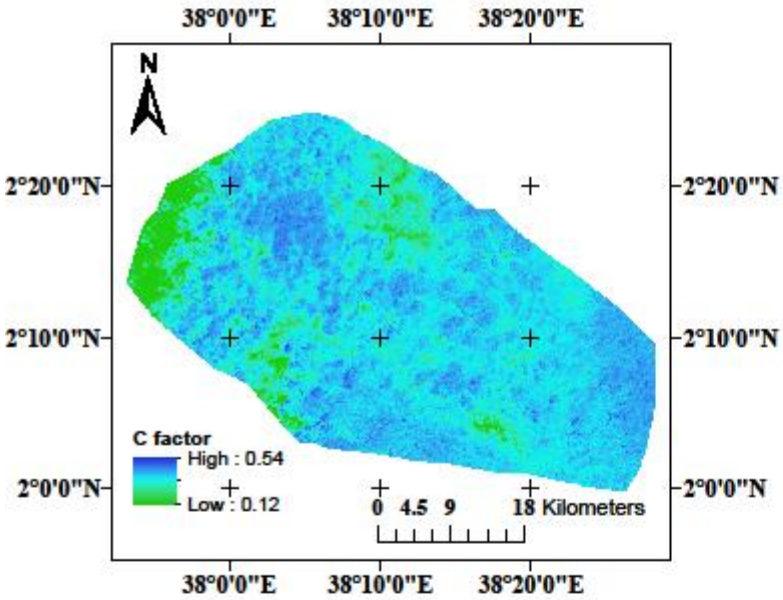

Figure 0.3. **Land cover factor map**

4.1.5 Model regression

The model regression was carried out with sampled data from simulated and observed soil loss data (Table 4.1). The model regression showed a close fit (Figure 4.4)

Table 0.1. Model Regression statistics

Regression Statistics	
Multiple F	0.97243
R Square	0.94562
Adjusted I	0.944189
Standard I	19.71657
Observati	40

ANOVA

	df	*SS*	*MS*	*F*	*gnificance F*
Regressio	1	256876.5	256876.5	660.7876	1.24E-25
Residual	38	14772.23	388.743		
Total	39	271648.8			

	Coefficients	*andard Err*	*t Stat*	*P-value*	*Lower 95%*	*Upper 95%*	*ower 95.0%*	*pper 95.0%*
Intercept	5.249953	13.68085	0.383745	0.703307	-22.4455	32.9454	-22.4455	32.9454
X Variable	0.951908	0.037031	25.70579	1.24E-25	0.876943	1.026873	0.876943	1.026873

RESIDUAL OUTPUT

PROBABILITY OUTPUT

Observatio	*Predicted Y*	*Residuals*	*dard Residuals*	*Percentile*	*Y*
1	227.0445	-22.0445	-1.13268	1.25	205
2	233.7078	-26.7078	-1.3723	3.75	207
3	233.7078	-21.7078	-1.11539	6.25	212
4	252.746	-34.746	-1.78531	8.75	218
5	252.746	-28.746	-1.47702	11.25	224
6	252.746	-21.746	-1.11735	13.75	231
7	266.0727	-28.0727	-1.44243	16.25	238
8	266.0727	-8.0727	-0.41479	18.75	258
9	267.9765	3.023484	0.155352	21.25	271
10	269.8803	11.11967	0.571348	23.75	281
11	277.4956	13.50441	0.693881	26.25	291
12	282.2551	9.744866	0.500709	28.75	292
13	286.0628	24.93723	1.28132	31.25	311
14	287.9666	28.03342	1.440407	33.75	316
15	296.5338	31.46625	1.616792	36.25	328
16	297.4857	32.51434	1.670645	38.75	330
17	300.3414	31.65862	1.626676	41.25	332
18	306.0528	29.94717	1.538739	43.75	336
19	310.8124	27.18763	1.396949	46.25	338
20	331.7543	27.24566	1.399931	48.75	359
21	343.1772	16.82276	0.864384	51.25	360
22	346.033	14.96704	0.769033	53.75	361
23	372.6864	-8.68638	-0.44632	56.25	364
24	393.6284	-24.6284	-1.26545	58.75	369
25	394.5803	-24.5803	-1.26298	61.25	370
26	396.4841	-20.4841	-1.05251	63.75	376
27	397.436	-0.43598	-0.0224	66.25	397
28	405.0512	-6.05124	-0.31092	68.75	399
29	416.4741	-7.47414	-0.38403	71.25	409
30	418.378	-4.37795	-0.22495	73.75	414
31	425.9932	-4.99322	-0.25656	76.25	421
32	426.9451	2.054875	0.105583	78.75	429
33	437.4161	-8.41611	-0.43243	81.25	429
34	438.368	-4.36802	-0.22444	83.75	434
35	446.9352	-3.93519	-0.2022	86.25	443
36	453.5985	2.401455	0.123391	88.75	456
37	459.31	3.690008	0.189599	91.25	463
38	476.4443	-3.44433	-0.17698	93.75	473
39	479.3001	1.699944	0.087346	96.25	481
40	479.3001	1.699944	0.087346	98.75	481

Figure 0.4. **A comparison of observed and simulated soil loss**

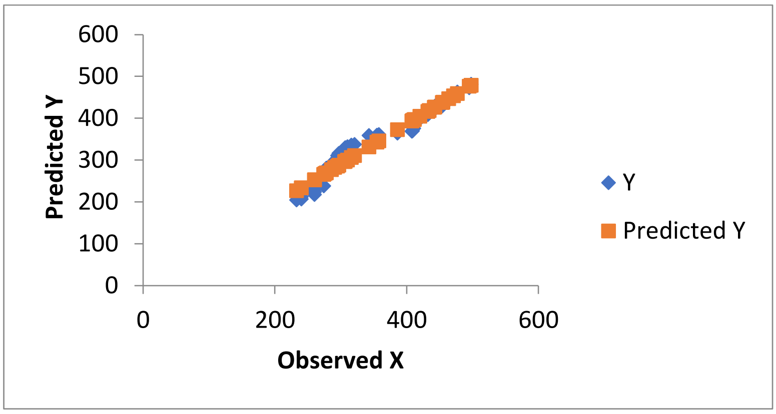

The model Nash Sutcliffe efficiency of 0.95 indicates a model with more predictive skills (Figure 4.5).

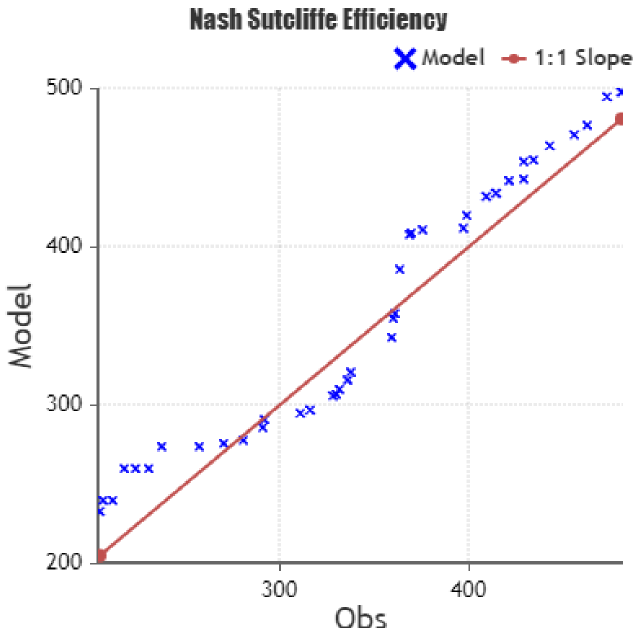

Figure 0.5. The NSE efficiency

The model correlation coefficient (R^2) of 0.95 (Figure 4.6) indicates a strong correlation between the observed and the predicted while the Pearson's coefficient (R) of 0.97 indicates a strong linear relationship between the predicted and the observed.

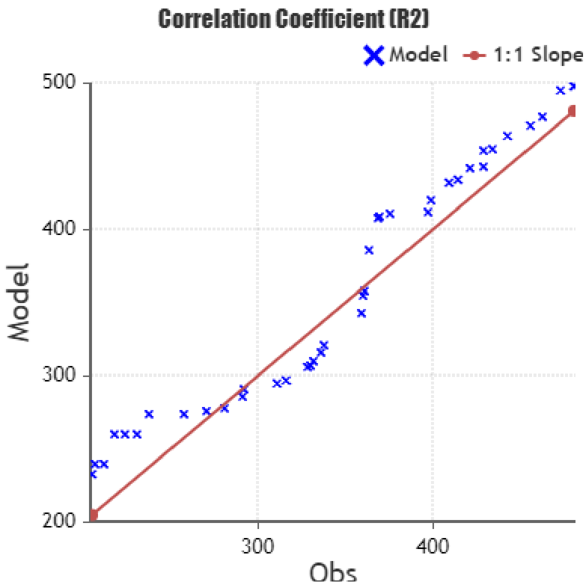

Figure 0.6. Correlation coefficient

4.2 Determination of spatial soil loss

The RUSLE input parameters were processed in the GIS environment to produce the five RUSLE factors after calibration and validation.

4.2.1 The R factor

The high and low rainfall amount were in high and lower parts of the catchment respectively. The highest and lowest rainfall factors were 460 and 201 respectively shown in the rainfall factor map (Figure 4.7).

4.2.2 The K factor

The maps representing the soil factor equation shown in RUSLE factors algorithms (Table 3.1) are described in the soil factor parameter (Table 4.2) and presented in the soil erodibility factor maps (Appendix II). The study area showed that the K factor ranged between 0.004 and 0.058 with a mean score of 0.045 and standard deviation of 0.015 as shown in the soil erodibility factor map figure 4.8. The predominant soil structure was code 3 and 4 described as fairly to slightly structured soil while the profile permeability predominantly was coded as 3 and 5 described as moderate to slow. The soil organic matter was below 1%. The major soil properties of the study are described in appendix VI.

4.2.3 The LS factor

The maps representing the LS factor equation shown in the RUSLE factors algorithms (Table 3.1) are described in the LS factor parameters (Table 4.3) and presented in the LS factor parameters appendix III, (Moore and Burch 1986a). The LS mean score was 1 with a standard deviation of 5 while the minimum and maximum was 0 and 231 respectively as shown in the slope length factor map (Figure 4.9).

4.2.4 The C factor

The maps representing the C factor equations shown in the RUSLE factors algorithms (Table 3.1) are described in the C factor parameters (Table 4.4) and presented in the C factor parameters maps appendix iv (University of Toronto, Admin 2015; Durigon ., 2014). The study area C factor values ranged between -0.045 and 0.58 with a mean score of 0.366 and standard deviation of 0.08 as shown in the land cover factor map (Figure 4.10).

4.2.5 The modified P factor

The land use map showing agricultural and non-agricultural areas and reclassified slope map of the study area (Figure A13) and (Figure A14) respectively are shown in the P factor maps (Appendix V). The P factor ranged from 0.10 to 1 with a mean value of 0.94 and standard deviation of 0.22 as shown in the practice factor map (Figure 4.11).

4.2.6 The soil loss (A)

The annual soil loss rate within the catchment was 279 t/ha (Figure 4.12).

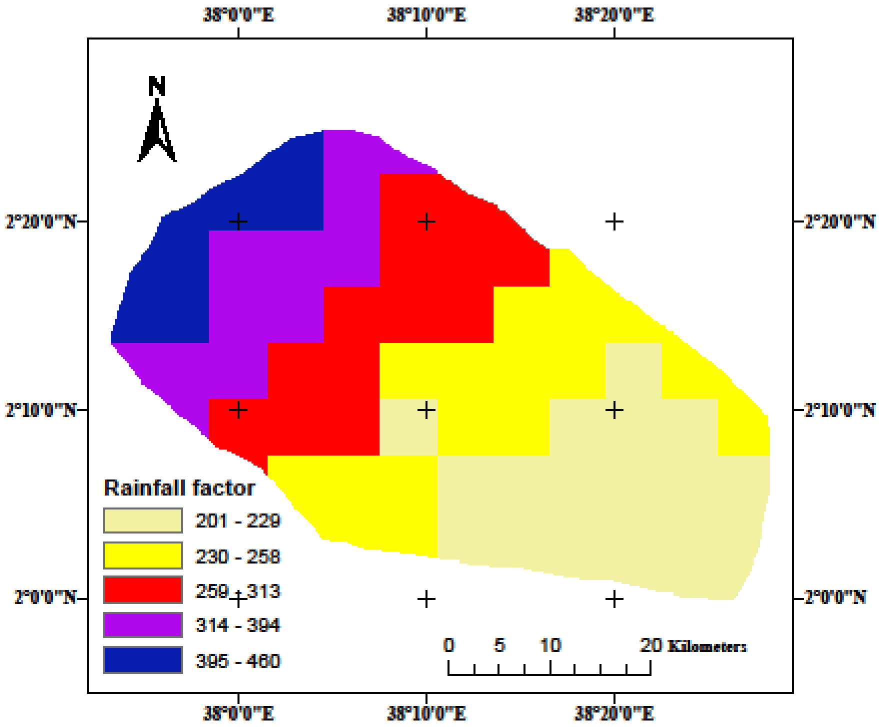

Figure 4.7. Rainfall factor map

Table 4.2. Soil factor parameters

No	Soil parameter	Description of the soil of the soil parameter
1	Silt figure A1	12.00 – 30.00 %
2	Sand figure A2	17.00 - 42.00 %
3	Clay figure A3	35.00 -70.00%
4	Soil organic matter figure A4	0.700 – 1.100%
5	Soil structure code figure A5	2, 3 and 4
6	Soil permeability code figure A6	2, 3 and 5

Table 0.3. Slope length (LS) factor parameters

No	LS parameter	Description of the LS parameter
1	Sink filled map – figure A7	326 -1681
2	Flow direction map – figure A8	1 - 65
3	Flow accumulation – figure A9	0 – 602,549 cells
4	Slope gradient – figure A10	0 – 58 degrees

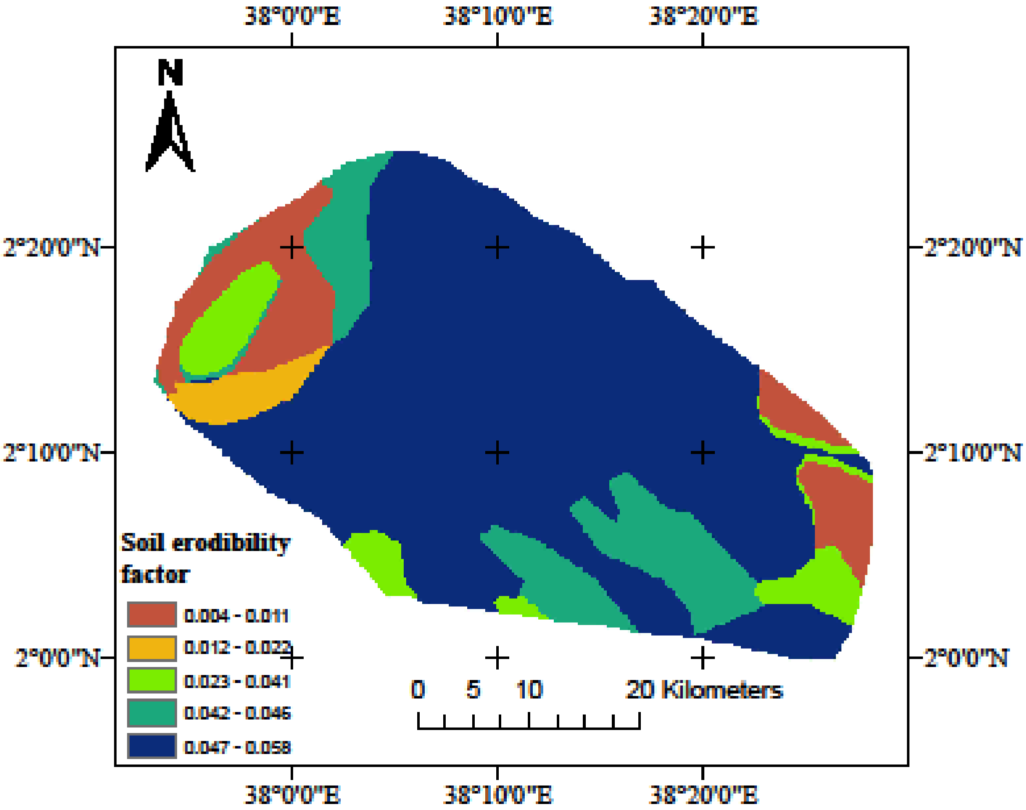

Figure 4.8. Soil erodibility factor map

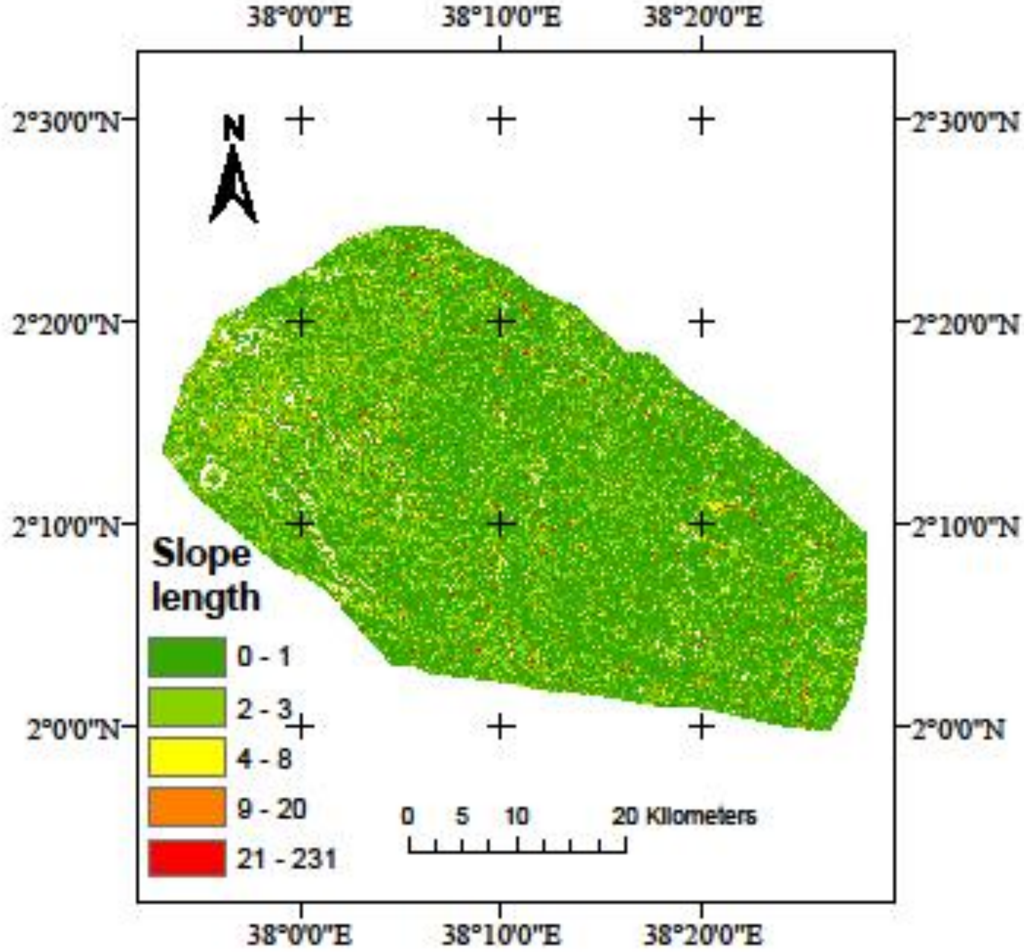

Figure 4.9. Slope length factor map

Table 4.4. C factor parameters

No	C-Parameter	Description of the C
1	Regional NDVI figure A11	-1.00 to 1.00
2	Study area NDVI figure A12	-0.08 to 0.55

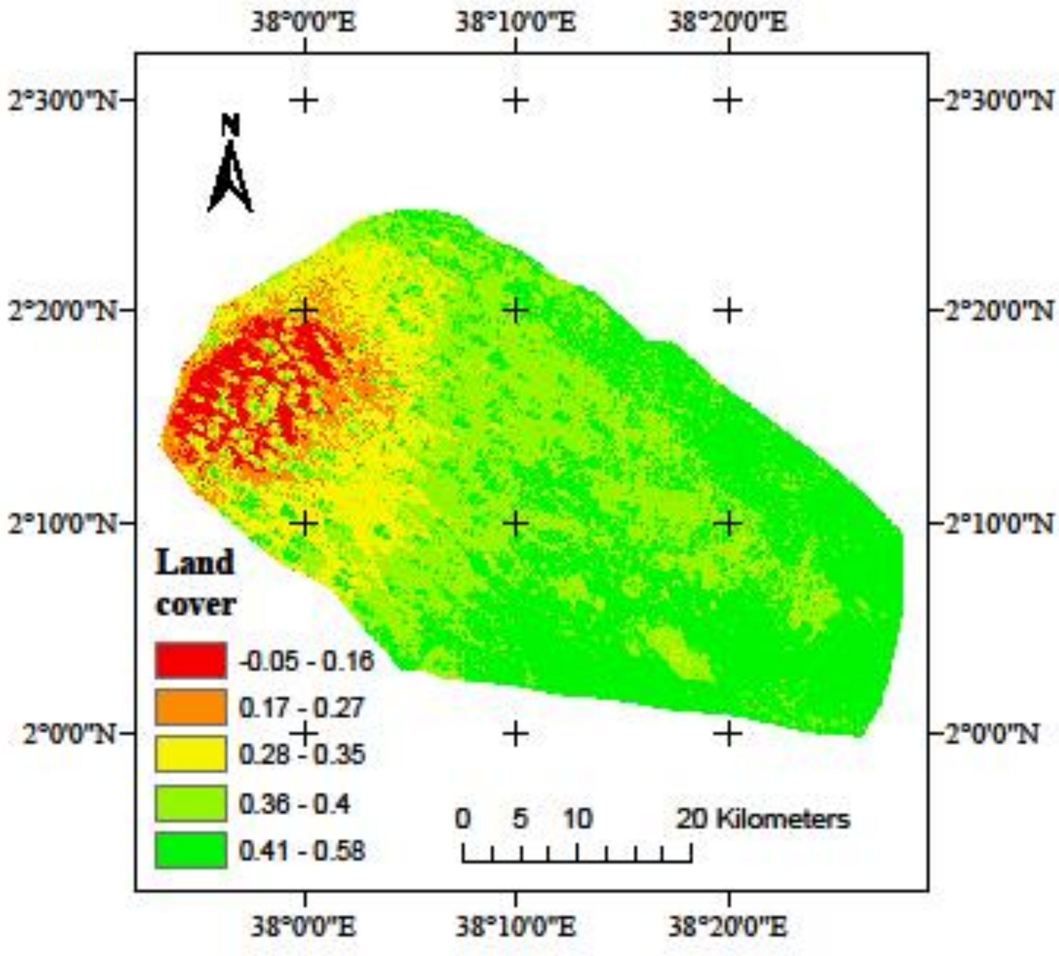

Figure 4.10: Land cover factor Map

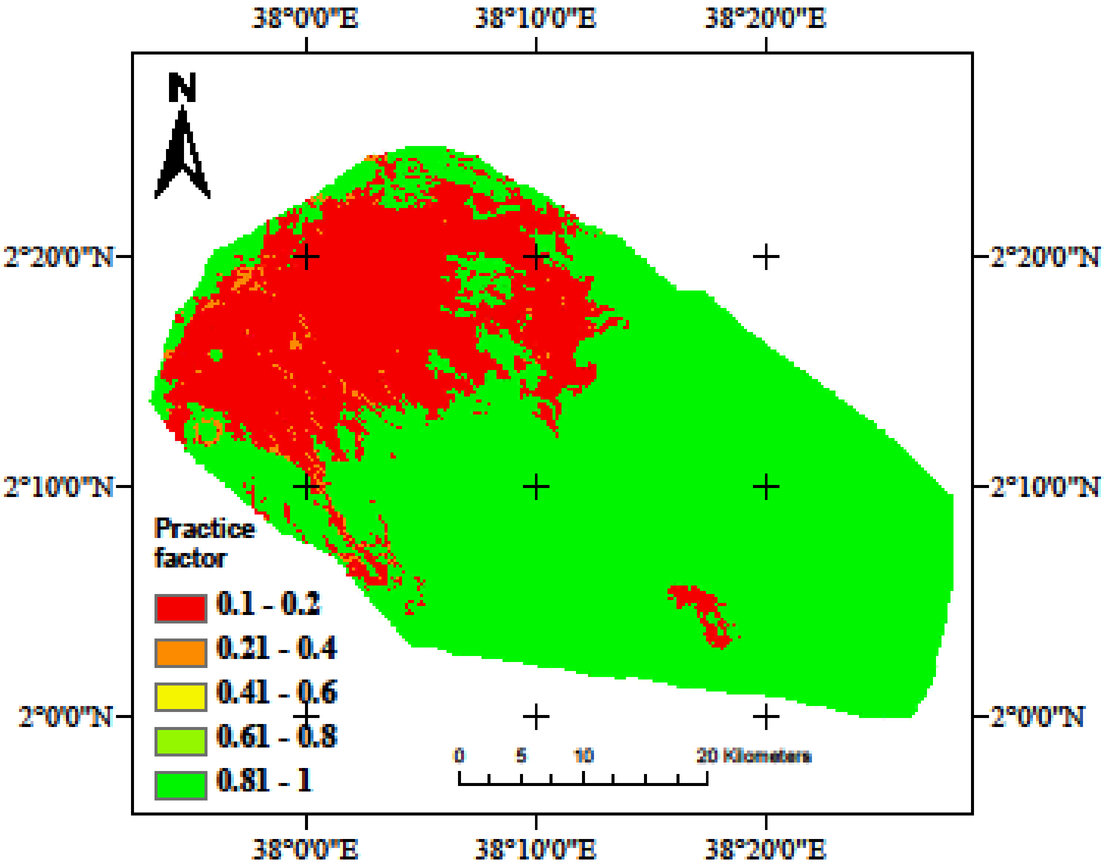

Figure 4.11. Practice factor map

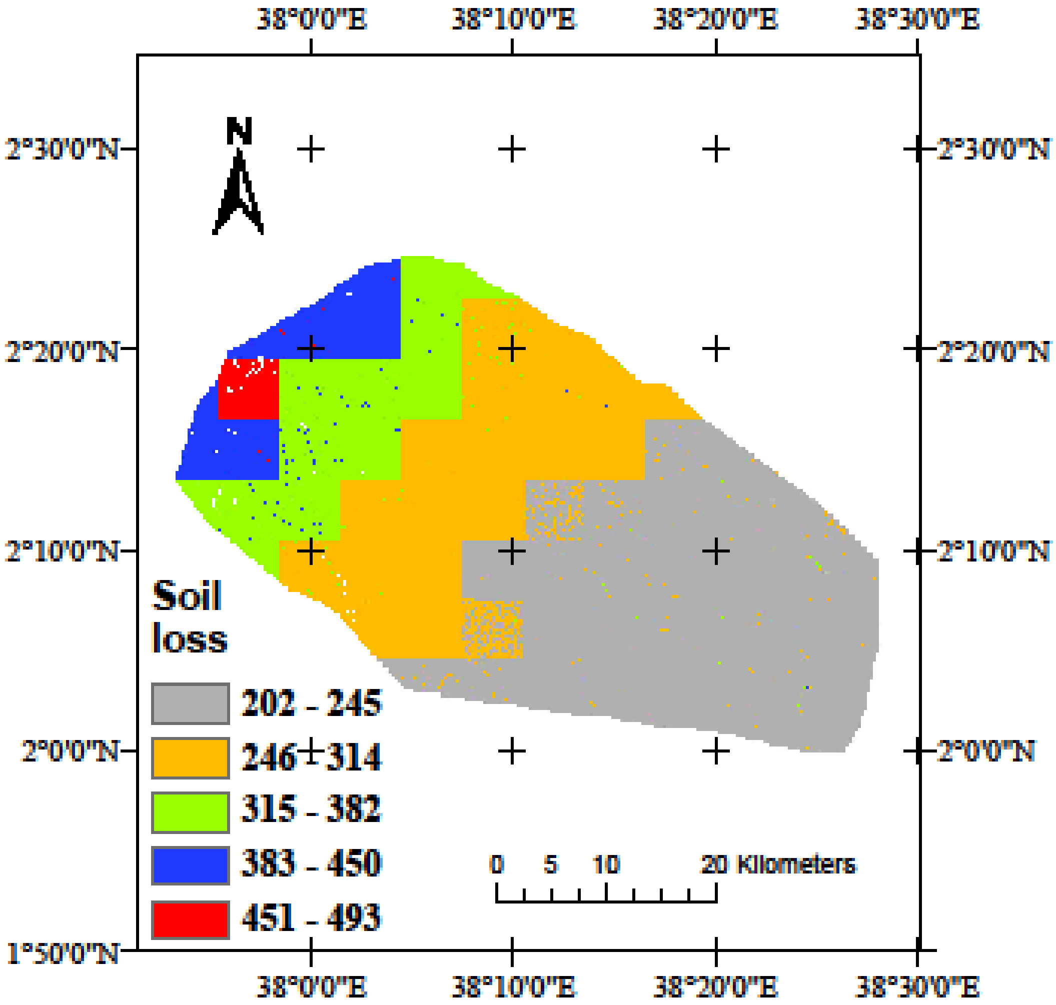

Figure 4.12. Soil loss map

4.3 Hypotheses testing

Table 0.5. ***Test parameters***

	Random
Mean	329.725
Variance	5407.64
Observations	40
Hypothesized Mean Difference	279
Df	39
t Stat	4.362628
P(T<=t) one-tail	4.56E-05
t Critical one-tail	1.684875
P(T<=t) two-tail	9.13E-05
t Critical two-tail	2.022691

The result showed that RUSLE simulation significantly produced non homogeneous soil loss within the catchment, $t\ (39) = 4.363$, $p < .001$.

4.4 Delineated erosion risk areas

The values of annual soil loss range within the study area are shown in Table 4.6. The lowest value is 202.00 t/ha while the highest value is 493.00 t/ha eroded from the area of 833.00 km^2 and 30.00 km^2 respectively. The study adopted the soil loss severity classes (Table 4.7), (Rahaman et al., 2015; Gizachew, 2015). From Table 4.5, 70% of the study area was classified under high erosion level while the remaining 30% was classified as severe.

Table 4.6. Range of area of annual soil loss values

No.	Annual soil loss range value (t/ha)	Area in Sq. km	Area in %
1	202.00 - 245.00	833.00	45.00%
2	246.00 - 314.00	551.00	30.00%
3	315.00 - 382.00	293.00	15.00%
4	383.00 - 450.00	142.00	8.00%
5	451.00 - 493.00	30.00	2.00%

Table 4.7. Soil loss severity classes

No	Annual soil loss range value (t/ha)	Soil loss severity classes	Area in Sq. km	Area in %
1	<10	Nil	0	0
2	10 – 50	Low	0	0
3	50 – 150	Moderate	0	0
4	150 – 300	High	1293	70%
5	>300	Severe	556	30%

CHAPTER 5: DISCUSSION

5.1 Model calibration and validation

The model calibration and validation showed strong correlation between the observed and simulated soil losses. The correlation coefficient (r) was 0.97 while the NSE was 95%. The strong correlation was attributable to both observed and simulated input data that was collected for the study area. The model can be adopted in the study area catchment with improvement involving high resolution data covering three parameters: soil, slope length, land cover while rainfall would require more rainfall stations.

5.2 Determination of soil loss using RUSLE

The RUSLE simulation produced the spatial soil loss within Golole catchment (Figure 4.12). The soil factor (K) result can be described as low (Figure 4.8). From the soil erodibility factor maps (Appendices II and Appendix VI), the soil physical characteristics can be described as having very low organic matter, slightly structured and belonging to a permeability class of slow to moderate. The presence of soil organic matter in the soil in varying degree increases soil porosity and capacity to hold water which in turn reduces soil erodability (Jankauskas et al., 2007). Information on soil's organic matter, structure and profile permeability class enhance erodibility prediction accuracy (Wischmeier and Smith, 1978).

Wischmeier and Smith (1978) found that soil erodibility was directly proportional to the silt fraction. Sand, sandy loam and loam soils are less erodible than silt, very fine sand and certain clay soils (Wischmeier and Mannering, 1969). The study area soil texture can be described as predominantly loamy clayey (Appendix VI). As clay fraction increases, erodibility decreases, a phenomenon attributable to the increased cohesiveness associated with clay soils (Wischmeier and Mannering, 1969).

The analysis conducted on both slope length and soil loss maps figures 4.9 and 4.12 respectively indicated a direct proportionality. In this case, the two were compared using similar coordinates and showed similar trends where high or low slope length factor meant high or low rate of soil loss. The high and low soil loss rates occurred in the highlands and lowlands respectively as shown in the soil loss map (Figure 4.12). The other researchers using RUSLE in a GIS environment in similar catchments got an annual average soil loss rate of 600 t/ha for Taita hills in Kenya (Mawasi, 2013), 93 t/ha from Chemoga Blue Nile Basin, Ethiopia (Bewket and Teferi, 2009) and 42 t/ha from cultivated fields in Ethiopia (Hurni, 1993). Hurni et al., (2008) confirmed the high soil loss in Ethiopia on test plots amounting to between 130 to 170 t/ha/yr. In Ethiopian highlands Abate (2011) established an annual soil loss of between 200 and 300 t/ha/yr., while Nkonya et al., (2016) found that in Ethiopia soil loss ranged between 42 and 300 t/ha/yr.

Ban *et al* (2016) demonstrated the advantage of using RS and GIS in estimating soil loss for Kulekhani catchment, Nepal where 58% of the catchment area was prone to high and very severe erosion with a mean annual soil loss of 195 t/ha/yr. The severe erosion rates occurred in hilly, steep and undulating terrains as shown by the slope length factor map and soil loss map (Figures 4.9 and 4.12).

A similar trend was noted using RUSLE and geo-information technology in a small sub-watershed in Kerala, India (Prasannakumar, 2011). The upper part of the catchment above 1100 m a.s.l., occupied by the forest was covered by thick vegetation mainly shrubs and trees as shown in plate 5.1. The forest area was hilly, with undulating terrain and home to wildlife (elephants, buffalos, monkeys, antelopes among others). Deforestation (cutting of trees) as well as human encroachment on the forest land was noted in areas bordering the forest. The cultivated land exhibited minimal vegetation cover (plate 5.2). Rills and gullies were observed on the terrains as shown in plate 5.3.

Plate 6.1. Marsabit forest. Photo taken from location: N02.22255, E037.96703, 1020 m a.s.l.

Plate 6.2. Farming land in Badassa without soil conservation measures.
Location: N02.26208 E038.01300, 1025m a.s.l.

Plate 6.3. Gully formation in a farmland in Songa. Location: 02.23835, E037.99631, 1006m a.s.l.

The surface water sources comprising of earth pans and dams were heavily silted due to the high amount of soil brought from the upper reaches of the catchment. Rills and gullies were observed on hilltops and on steep slope terrains. In the cultivated areas few farms used stone contour ridges. The rangelands occupying the lowland plains had vegetation depleted to minimal vegetation and bare land due to overgrazing.

5.3 Delineation of risky areas of soil erosion

The soil loss within the catchment varied significantly from one area to another and therefore the soil loss was not homogeneous. The study delineated risk areas of soil erosion according to soil loss severity classes (Table 4.7) where 30% of the study area land mass experienced severe soil loss rates.

The study acknowledges that the entire catchment was prone to accelerated erosion since the minimum annual soil loss rate of 202 t/ha was above the recommended annual soil erosion tolerable level of 4.8 t/ha for the area (Sombroek et al., 1980).

RUSLE factors are classified into two categories; environmental and management with the former remaining relatively constant over time while the latter varies considerably (Rahaman et al., 2015). This implies that the management factors affecting both land cover and land use can be manipulated considerably to reduce the rate of the soil loss. Bonarius (1975) cautioned that cultivation on the eastern slopes of Mt. Marsabit especially below 1,300 m a.s.l. should be reduced to curb soil erosion hazard (Bonarius, 1975).

During ground truthing, minimal land cover was observed in the cultivated areas that also exhibited high soil loss. This study found that lack of vegetation cover and type of land use (cultivation and grazing) were the main contributors to the severe and high rate of soil loss in the study area.

The high rate of soil erosion in Marsabit mountain ecosystem (highlands) occurred in areas with less or no vegetation cover (Okoth, 2006). The results showed that land cover (C factor) and land use (P factor) comprised of the management factors that could be economically manipulated through conservation measures to greatly reduce soil loss (Renard *et al*., 1995).

The findings in this study agree with the observation that the high rates of erosion in Ethiopia was caused by: deforestation, overgrazing, detrimental cultivation practices, poverty, land fragmentation and expansion of cropland (Birham, 2016).

CHAPTER 6: CONCLUSIONS AND RECOMMENDATIONS

6.1 **Conclusion**

The result from this study based on the objectives and the hypotheses affirmed that RUSLE simulation:

1. Generated the spatial soil loss within Golole catchment hence the study determined the spatial soil loss.
2. Generated a non-homogeneous soil loss within Golole catchment hence the study delineated risky areas of soil erosion.

6.2 Recommendations

This study recommends the following:

1. Further research on RUSLE simulation coupled with calibration and validation using high resolution data.
2. Further research on RUSLE simulation on temporal trends of the soil erosion hazard using high resolution data.
3. This study recommends further research in the forest reserve areas that showed the greatest rates of soil erosion menace to determine underlying causes and appropriate soil erosion mitigation measures.

REFERENCES

Abate, S. (2011). Estimating soil loss rates for soil conservation planning in the Borena Woreda of South Wollo highlands, Ethiopia: The Case from the Legemara Watershed. *Journal of Sustainable Development in Africa,* 13(3). Retrieved from http://www.jsdafrica.com/Jsda/V13No3_Summer2011_A/PDF/Estimating20Soil20Loss20Rates20for20Soil20Conservation20Planning20in20the20Borena20Woreda.pdf

Adediji, A., Tukur, A., & Adepoju K. (2010). Assessment of Revised Universal Soil Loss Equation (RUSLE) in Katsina area: Katsina State of Nigeria using Remote (RS) and Geographic Information System (GIS). *Iranica Journal of Energy & Environment* 1 (3)*:* 255-264.

Agricultural and Meteorological software (2019). Online Calculators. Available on: https://agrimetsoft.com/calculators/Nash%20Sutcliffe%20model%20Efficiency%20coefficient

University of Toronto Admin, (2015). Calculating vegetation indices from Landsat image using ArcGIS 10.1: School of the Environment University of Toronto. Retrieved from http://grindgis.com/blog/vegetation-indices-arcgis.

Adhikari, K. & Hartemink, A. (2016). Linking soils to ecosystem services - A global review. Geoderma. DOI: 10.1016/J.GEODERMA.2015.08.009.

Angima, S., Stott, D., O'Neill, M., Ong, C., & Weesies, G. (2003). Soil erosion prediction using RUSLE for central Kenyan highland conditions. *Agricultural, Ecosystems and Environment, 97(*1-3*),* 295-308, doi: 10.1016/S0167-8809(03)00011-2

Ashiagbor, G., Forkuo, K., Laari, P., & Aabeyir, R. (2013). Modeling soil erosion using RUSLE and GIS tools. International Journal of Remote Sensing & Geoscience (IJRSG). Volume 2. 7-17.

Ban, J., Yu, I., & Jeong, S. (2016). Estimation of Soil Erosion Using RUSLE Model and GIS Techniques for Conservation Planning from Kulekhani Reservoir Catchment, Nepal. Journal of Korean Society of Hazard Mitigation. 16. 323-330, doi: 10.9798/KOSHAM.2016.16.3.323.

Borrelli, P., Robinson, D., Fleischer, L., Lugato, E., Ballabio, C., Alewell, C. Panagos, P. (2017). An assessment of the global impact of 21st century land use change on soil erosion. Nature Communications, doi: org/10.1038/s41467-017-02142-7

Baldock A., & Nelson N. (2000). *Soil organic Matter*: Handbook of soil science, chapter 2, CRC Press, Boca Raton, FL, B25–B84, doi: 10.1038/194324b0

Beskow, S., Mello, C., Norton, L., Curi, N., Viola, M., & Avanzi J. (2009). Soil erosion prediction in the Grande River basin, Brazil using distributed modeling. *Catena* 79(1), 49-59.

Bewket, W., & Teferi, E. (2009). Assessment of soil erosion hazard and prioritization for treatment at the watershed level: A case study in the Chemoja watershed, Blue Nile basin, Ethiopia. *Land Degradation and Development: Wiley InterScience, 20:* 609–622. doi:10.1002/ldr.944

Birham, A. (2016). Quantification of soil loss using GIS and Remote Sensing in Northern Ethiopia. *Esri Eastern Africa Education GIS conference, Addis Ababa,* 23-24 September 2016, 126-136.

Biswas, S. & Pani, P. (2015). Estimation of soil erosion using RUSLE and GIS techniques: a case study of Barakar River basin, Jharkhand, India. *Model. Earth Syst. Environ.* **1,** 42 (2015), doi.org/10.1007/s40808-015-0040-3.

Bonarius, H. (1975). Kenya soil survey, preliminary assessment of irrigation development in the Marsabit area: Special Task Force, Minor Irrigation Development, Ministry of Agriculture, Republic of Kenya. *Scanned from Original by ISRIC-World Soil Information, as ICSU, World Data Centre for soil.* Retrieved from *https://library.wur.nl/isric/fulltext/isricu_i00002781_001.pdf*

Carlos, A., Bonilla, Jose L., Reyes, & Magri, A. (2010). Water erosion prediction using the Revised Universal Soil Loss Equation (RUSLE) in a GIS framework, Central Chile. *Chilean Journal of Agricultural Research,* 70(1), 159-169.

Carvalho, D., Durigon, V., Antunes, M., Almeida, W., & Oliveira, P. (2014). Predicting soil erosion using RUSLE and NDVI time series from TM Landsat 5. *Pesquisa Agropecuária Brasileira. 49*(3), 215 –224, doi: 10.1590/S0100-204X2014000300008.

Dominik, F., Robert, B., Malcolm, M., Manfred, M., Mathias, V., Tim, R., Julia, E., & Stephen E. (2007). East Africa soil erosion recorded in a 300-year-old coral colony from Kenya. Geographical research letters: Vol. 34, L04401, doi: 10.1029/2006gL028525.

Durigon, V., Carvalho, D., Antunes, M., Oliveira, P., Fernandes, M. (2014). NDVI time series for monitoring RUSLE cover management factor in a tropical watershed. *International Journal of Remote Sensing*. *35*(2). 441-453. 10.1080/01431161.2013.871081.

FAO, (2019). Global symposium on soil erosion (GSER 19).

FAO, IFAD & WFP. (2015). The State of Food Insecurity in the World. Meeting the 2015 international hunger targets: taking stock of uneven progress. Rome, FAO.

FAOSTAT. (2005). Food and Agricultural Organization of the United Nations Statistical Databases. Rome: FAO.

FAO, & ITPS. (2015). Status of the World's Soil Resources (SWSR) – Main Report. Food and Agriculture Organization of the United Nations and Intergovernmental Technical Panel on Soils, Rome, Italy.

FAO. (2019). Proceedings of the Global Symposium on Soil Erosion. Rome.

Fistikoglu, O., & Harmancioglu, N. (2002). Integration of GIS with USLE in assessment of soil erosion. *Water resources management 16*(6) 447- 476, doi: 10.1023/a: 1022282125760.

Foster, G., Toy, T., and Renard K. (2003). Comparison of the USLE, RUSLE 1 and RUSLE 2 for application in the highly disturbed lands. US Department of Agriculture (USDA), Agricultural Research Service (ARS): First Interagency Conference in the Watersheds, 27-30 October 2003. Retrieved from https://www.tucson.ars.ag.gov/ICRW/Proceedings.htm

Ganasri, B., Ramesh, H. (2015). Assessment of soil erosion by RUSLE model using remote sensing and GIS - A case study of Nethravathi Basin, Geoscience Frontiers. http://dx.doi.org/10.1016/j.gsf.2015.10.007

Government of Kenya. (2016). Land degradation assessment in Kenya.

Government of Kenya. (2013). Kenya National Environment Policy.

Gunter, B. (2006). Rainfall runoff modelling of ungauged catchments. Encyclopedia of Hydrological Science. John Wiley & Sons Ltd, doi: 10.1002/0470848944.hsa140.

Gizachew, A. (2015). A Geographical information system-based soil loss and sediment estimation in Zingin watershed for conservation planning, highlands of Ethiopia. *International Journal of Science, Technology and Society, 3(*1), 28-35, doi: 10.11648/j.ijsts.20150301.14.

Hussain I., & Misra U. (2018). Soil Loss Estimation in GIS Framework: A case study in Champabati watershed. Ijirae. *International journal of innovative research in advanced engineering, volume v*, 187-196, doi://10.26562/IJIRAE.2018.MYAE10090

Hudson, F. (2005). Soil Erosion Modelling using the Revised Universal Soil Loss Equation (RUSLE) in drainage basin in Eastern Mexico. *Environmental GIS: GRG* 360G.

Hurni, H. (1985). Soil conservation manual for Ethiopia. Ministry of Agriculture, Addis Ababa.

Hurni, H. (1993) Land Degradation, Famine and Resource Scenarios in Ethiopia. In: Pimentel, D., Ed., World Soil Erosion and Conservation, *Cambridge University Press,* Cambridge, 27-62. doi:10.1017/CBO9780511735394.004

Hurni H., Herweg K., Portner B., & Liniger H. (2008). Soil Erosion and Conservation in Global Agriculture. In: Braimoh A.K., Vlek P.L.G. (eds.) Land Use and Soil Resources. Springer, Dordrecht. doi.org/10.1007/978-1-4020-6778-5_4

Igwe, C., Akamigbo, F. & Mbagwu, J. (1999). Application of SLEMSA and USLE erosion models for potential erosion hazard mapping in south-eastern Nigeria. Int. Agrophys., 13(1), 41-48.

International Livestock Research Institute (ILRI, 1998). GIS Services. Website. Retrieved August 23 2016 from http://192.156.137.110/gis/postdownload.asp?dfile=zipfiles/kenya/Kenya_climate_surface.zip.

Ishtiyaq, A., & Verma M. (2013). Application of USLE model & GIS in estimation of Soil erosion for Tandula Reservoir. *International Journal of Emerging Technologies and Advanced Engineering, 3*(4), 570-576.

Jankauskas, B., Jankauskiene, G., & Fullen, M. (2007). Relationship between soil organic matter content and soil erosion severity in Albeluvisols of the Zemaiciai Uplands. *Ekologija, 53*(1), 21- 28.

Jeff, B. (2003). Eroding food security: linking soil erosion, soil fertility and crop yield in Kenya. Web site. Retrieved November 15, 2015. http://www.ieca.org/membersonly/cms/content/Proceedings/Object388PDFEnglish.pdf

Joy, T., & Muthukrishna, V. (2018). Assessing Non-Point Source Pollution Models: a Review. Vol. 27, No. 5 (2018), 1913-1922, doi: 10.15244/pjoes/76497.

Karuku, G. (2018). Soil and Water Conservation Measures and Challenges in Kenya; a Review. Current Investigations in Agriculture and Current Research. 2, doi:10.32474/CIACR.2018.02.000148.

Kenya Meteorological Department. (2016). *Rainfall data, Nairobi.*

Kenya National Population and Housing Census. (2009). *Population data, Nairobi.*

Kiage, L. M., Liu, K. B., Walker, N. D., Lam, N., & Huh, O. K. (2007). Recent land-cover/use change associated with land degradation in the Lake Baringo catchment, Kenya, East Africa: evidence from Landsat TM and ETM+. International Journal of Remote Sensing, 28(19), 4285–4309.

Kumar, A., Devi, M. & Deshmukh, B. (2014). Integrated Remote Sensing and Geographic Information System Based RUSLE Modelling for Estimation of Soil Loss in Western Himalaya, India. *Water Resource Manage* **28,** 3307–3317, doi: org/10.1007/s11269-014-0680-5

Mawasi, N. (2013). *Risk Assessment Analysis of Soil Erosion Using Geographic Information System (GIS) (*A case study of Taita Hills, Department of Geospatial and Space Technology, University of Nairobi, Nairobi, Kenya).

Mbugua, W. (2009). *Using GIS Techniques to Determine RUSLE's R and LS Factors for Kapingazi River Catchment (*Master of science research project report, Jomo Kenyatta University of Agriculture and Technology, Kenya). Retrieved from: http://citeseerx.ist.psu.edu/viewdoc/download;jsessionid=06915738208472B183C24BB177EE60ED?doi=10.1.1.603.9304&rep=rep1&type=pdf

Moses, A. (2017). GIS-RUSLE Interphase Modelling of Soil Erosion Hazard and Estimation of Sediment Yield for River Nzoia Basin in Kenya. J Remote Sensing & GIS 6: 205, doi: 10.4172/2469-4134.1000205

Moore, I., & Burch, G. (1986a). Physical Basis of the Length Slope Factor in the Universal Soil Loss Equation. *Soil Science Society of America, 50*(5), 1294 - 1298, doi:10.2136/sssaj1986.03615995005000050042x

Moore, I., & Burch, G. (1986b). Modeling erosion and Deposition: Topographic Effects. *Transactions of American Society of Agriculture and Biological Engineering, St. Joseph, Michigan, 29*(6), 1624 –1630, doi:10.13031/2013.30363

Morgan, R., Quinton, J., Smith, R., Govers, G., Poesen J., Auerswald, K., Styczen M. (1998). The European soil erosion model (EUROSEM): A dynamic approach for predicting sediment transport from fields and small catchments.

Nkonya, E., Mirzabaev, A., & Braun, J. (2016). Economics of Land Degradation and Improvement – A Global Assessment for Sustainable Development. Heidelberg etc.: 33-54

Obeta, I., & Adewumi J. (2013). Soil loss in Samaru Zaria Nigeria: A comparison of WEPP and EUROSEM models. Nigeria journal of Technology (NIJOTECH). 32(2). 197 – 202.

Okoth, E. (2006). *Characterization and assessment of erosion susceptibility of the soils of Mount Marsabit ecosystem* (Master's thesis). University of Nairobi, Kenya.

Panagos, P., Borreli P., Meusburger K., Zanden E., Poesen J., & Alewell C. (2015). Modelling the effect of support practices (P-factor) on the reduction of soil erosion by water at European scale. *Environmental Science and policy, 51,* 23-34, doi.org/10.1016/j.envsci.2015.03.012

Phinzi K., & Ngetar N. (2017). Mapping Soil Erosion in a Quaternary Catchment in Eastern Cape Using Geographic Information System and Remote Sensing. *South African Journal of Geomatics, 6. No. 1.* DOI: http://dx.doi.org/10.4314/sajg.v6i1.2

Prasannakumar, V., Vijith, H., & Geetha, N. (2011). Estimation of soil erosion risk within a small mountainous sub-watershed in Kerala, India, using Revised Universal Soil Loss Equation (RUSLE) and Geo-Information Technology. *Geoscience Frontiers, 3*(2), 209-215,

doi: 10.1016/j.gsf.2011.11.003

Prasannakumar V., Vijith H., Abinod S., & Getha N. (2015). Estimation of soil erosion risk within a small mountainous sub-catchment in Kerala, India, using RUSLE and geo-information technology. *Geoscience Frontiers* 3(2), 2012 209e.

Pushpalatha, K., Kumar, K., Rao R., & Rejani R. (2017). Spatial and Temporal Variation of C– Factor and Soil Erosion in a Semi-Arid Watershed: A Case Study in Mahabubnagar District. *International Journal of Agricultural Science and Research (IJASR). 7*. 175-188,

doi: 10.24247/ijasroct201724

Rahaman, S., Aruchamy, S., Jegankumar, R., & Ajeez, S. (2015). Estimation of annual average soil loss based on RUSLE model in Kallar watershed, Bhavani Basin, Tamil Nadu, India. *ISPRS Annals of the photogrammetry, Remote sensing and spatial information sciences, II*(2/W2), 207-2014. Retrieved from https://www.isprs-ann-photogramm-remote-sens-spatial-inf-sci.net/II-2-W2/207/2015/isprsannals-II-2-W2-207-2015.pdf

Regional Centre for Mapping of Resources and Development (2016). *Landsat images*. Nairobi, Kenya.

Renard, K., Foster, G., Weesies, G., Mcool, D., & Yoder, D. (1995). The Revised Universal Soil Loss Equation. Department of defense / Interagency Workshop on Technologies to Address Soil Erosion on Department of Defense Lands San Antonio, Tx.

Renard, K., Foster, G., Weesies, G., Mcool, D., & Yoder, D. (1997). *Predicting soil erosion by water: A guide to conservation planning with the Revised Universal Soil Loss Equation (RUSLE): US Department of Agriculture, Agriculture Handbook N0. 703.* US government printing office, Washington, DC. 20402-9328. Retrieved from https://www.ars.usda.gov/ARSUserFiles/64080530/RUSLE/AH_703.pdf

Renard, K., Yoder, D., Lightle, D., & Dabney S. (2010). Universal Soil Loss Equation and Revised Universal Soil Loss Equation. Retrieved from https://www.tucson.ars.ag.gov/unit/publications/pdffiles/2122.pdf

Sanchez, P. (2002). Ecology: Soil fertility and hunger in Africa. *Science, 295*(5562), 2019-2020, doi: 10.1126/science.1065256

Shi, Z., Cai, C., Ding, S., Wang, T., & Chow, T. (2003). Soil conservation planning at the small watershed level using RUSLE with GIS: A case study in the three Gorge Area of China. *Catena 55*(2004), 33-48, doi: 10.1016/S0341-8162(03)00088-2

Smith, H. (1999). Application of Empirical Soil Loss Models in southern Africa: a review, South African Journal of Plant and Soil, 16:3, 158-163, DOI: 10.1080/02571862.1999.10635003 To link to this article, doi:10.1080/02571862.1999.10635003

Silburn, D., & Lock, R. (1989). Evaluation of the CREAMS model sensitivity analysis of the soil erosion sedimentation for aggregated clays.

Sombroek, W., Braun, H., & Pouw, B. (1980). *Exploratory soil map and agro-climatic zone map of Kenya: Exploratory soil survey report no. E1*. Nairobi.

Tamene L., Bao Q., & Vlek P. (2014). A Landscape Planning and Management Tool for Land and Water Resources Management: An Example Application in Northern Ethiopia. *Water Resource Manage, 28*:407–424, doi: 10. 1007/s11269-013-0490-1

Toy, T., Foster, G., & Renard, K. (2002). *Soil erosion processes, prediction, measurement, and control.* John Wiley & Sons, New York, NY.

Torsten, S., & Jannes, S. (2014). Applied comparison of the erosion risk models EROSION 3D and LISEM for a small catchment in Norway. *Catena 118*(2014), 154-167. doi.org/10.1016/j.catena.2014.02.004.

United States Geological Survey (USGS), (2016). Aster digital elevation model (DEM) Resolution of 30 Metres. Retrieved from https://gdex.cr.usgs.gov/gdex/

Wischmeier, W., & Mannering, J. (1969). Relation of soil properties to its erodibility. *Soil Science Society of America Proceedings, 33*(1), 131-137, doi:10.2136/sssaj1969.03615995003300010035x

Wischmeier, W., & Smith, D. (1978). *Predicting rainfall erosion losses*: *A guide to conservation planning agricultural handbook* no. 537. Science and education administration, US Department of Agriculture, Washington, DC. Retrieved from https://naldc.nal.usda.gov/download/CAT79706928/PDF

Yahya, F., Dalal Z., & Ibrahim F. (2013). Spatial estimation of soil erosion risk using RUSLE approach, RS, and GIS techniques: A case study of Kufranja catchment, Northern Jordan. *Journal of Water Resource and Protection, 05*(12), 1247-1261, doi:10.4236/jwarp.2013.512134

Yang, D., Kanae S., Oki T., Koike T., Musuake K. (2003). Global potential soil erosion with reference to land use and climate. *Wiley InterScience, 17*(14): 2913-2928. doi:10.1002/hyp.1441

APPENDICES

Appendix I: Kenya ecological zones

Kenya is divided into five altitude zones and seven moisture availability zones. The annual rainfall divided by potential evaporation gives moisture availability. The altitude zones are sea level to 200m, 200 – 1500m, 1500-2500m, 2500-3000m and >3000m. The moisture availability zones include very arid (zone VII), arid (Zone VI), semi-arid (zone V), semi-humid to semi-arid (zone IV), semi-humid (zone III), sub-humid (zone II) and humid (zone I). Areas designated as I, II and III with a moisture index greater than 50% have a high potential for cropping (Sombroek et al., 1980). *The* high agricultural potential areas are located above 1200 m altitude with a mean annual temperature of below 18°C while 90% of the semi-arid and arid zones lie below 1200 m a.s.l with a mean annual temperature ranging from 22° to 40°C.

Table A1. Kenya's ecological zones

ZONE	CLASSIFICATION	MOISTURE %	ANNUAL RAINFALL	% OF KENYA'S AREA
1V	Semi-humid to semi-arid	40 -50	600 -1100	5
V	Semi-arid	25 -50	450 - 900	22
VII	Very arid	<15	150 - 350	46

[1]Kenya's four out of seven ecological zones whose moisture index falls below 50%. [2]Target research area falls under semi humid to semi-arid: Source: Sombroek *et al*. (1980).

Appendix II: Soil erodibility factor maps

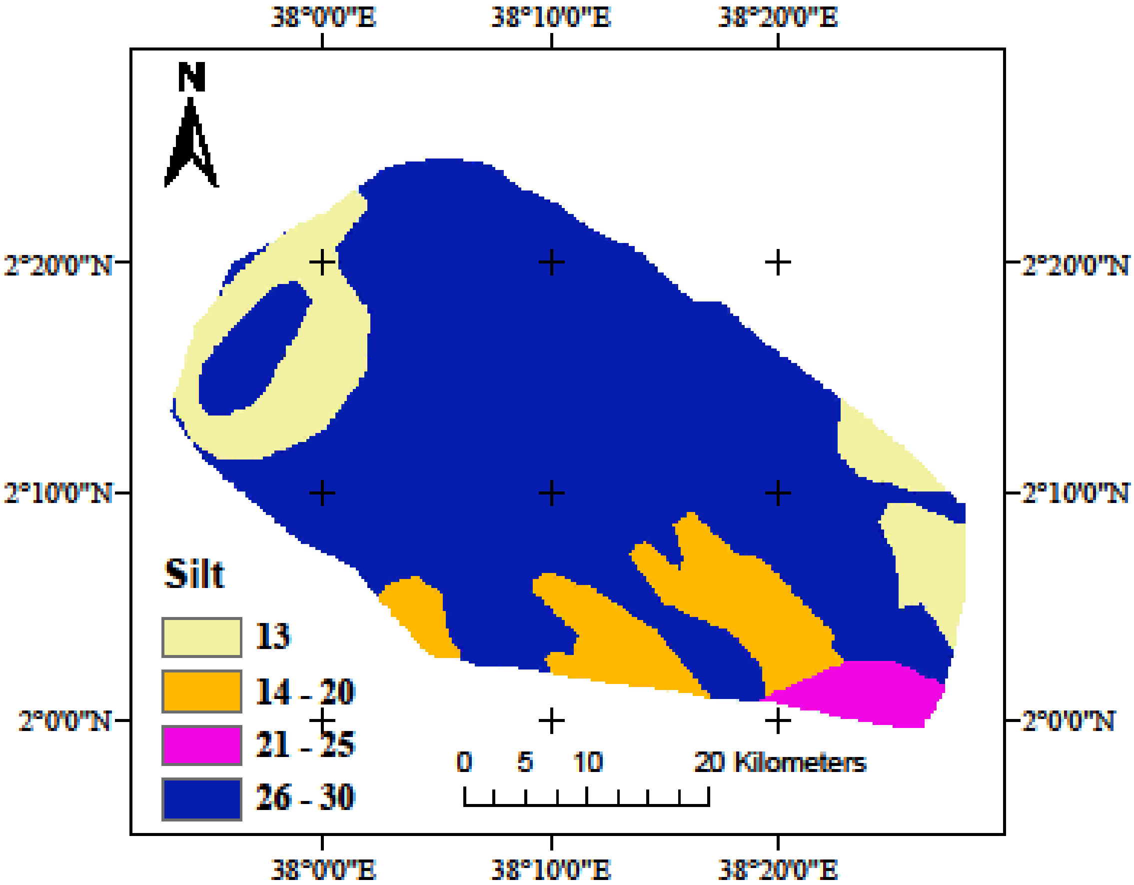

Figure A1. Percentage silt map

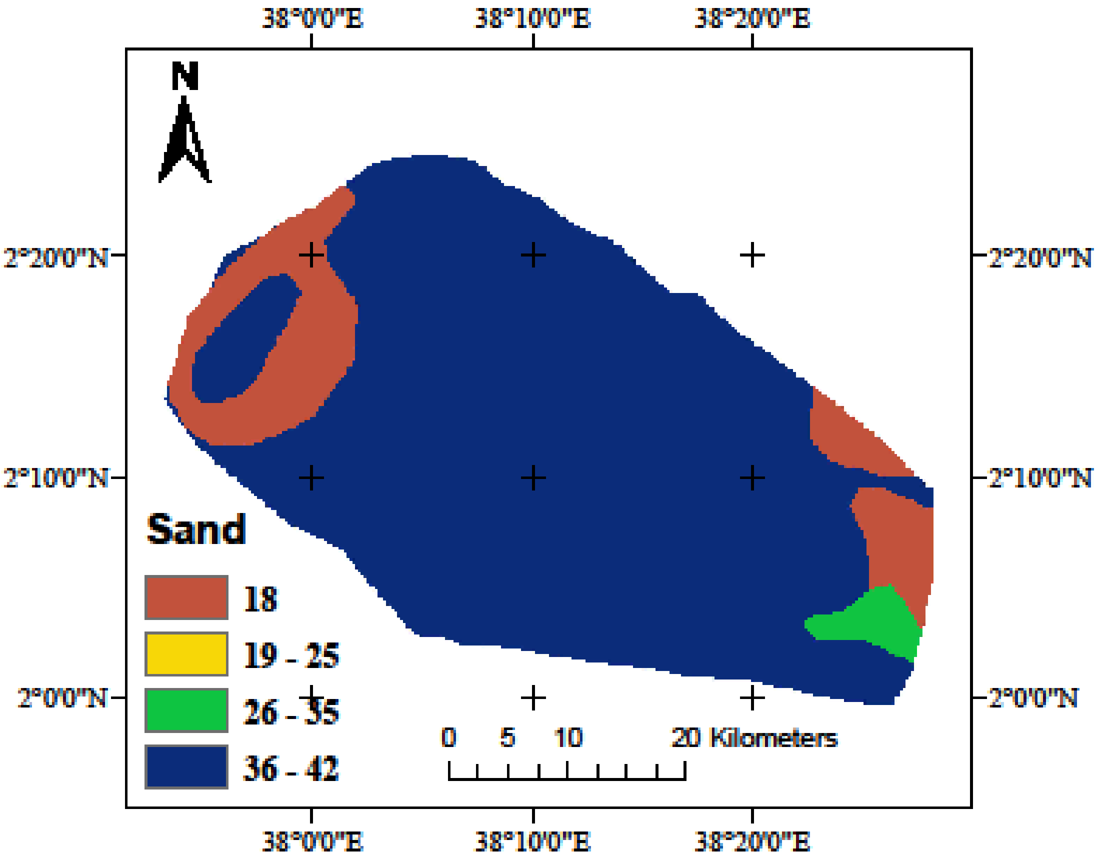

Figure A2. Percentage sand map

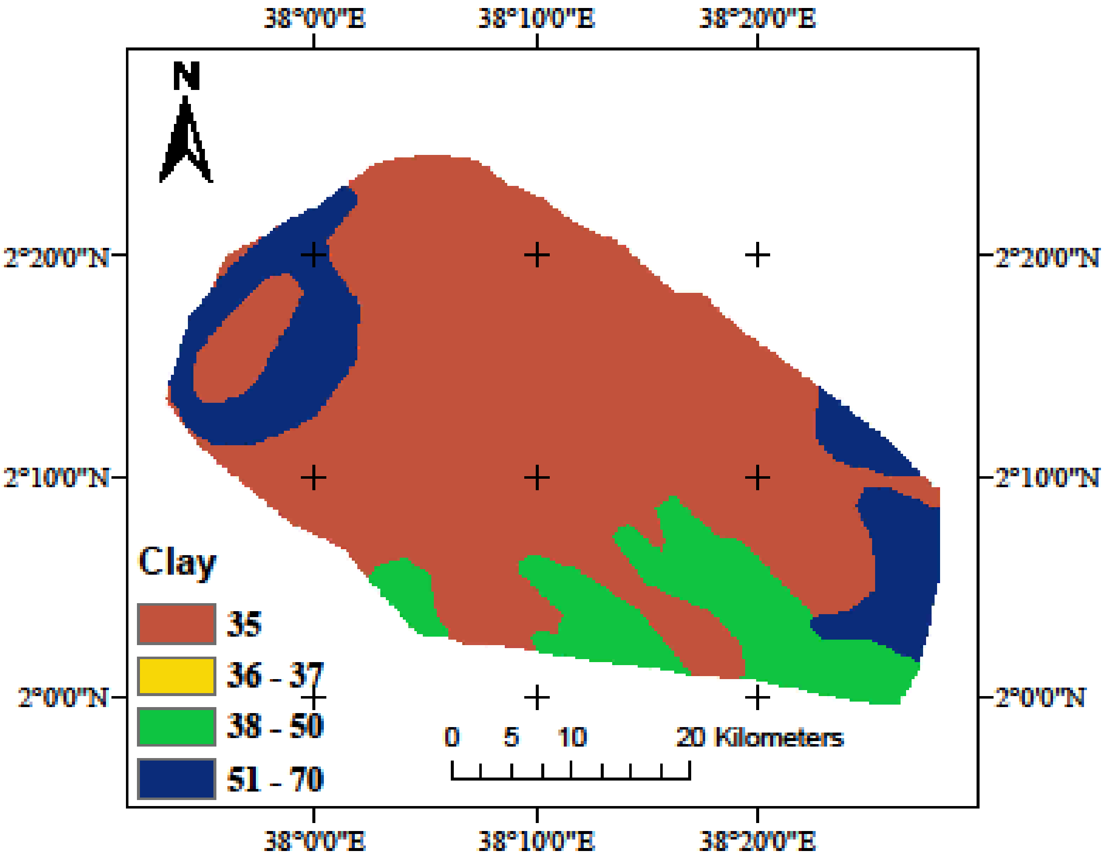

Figure A3. Percentage clay map

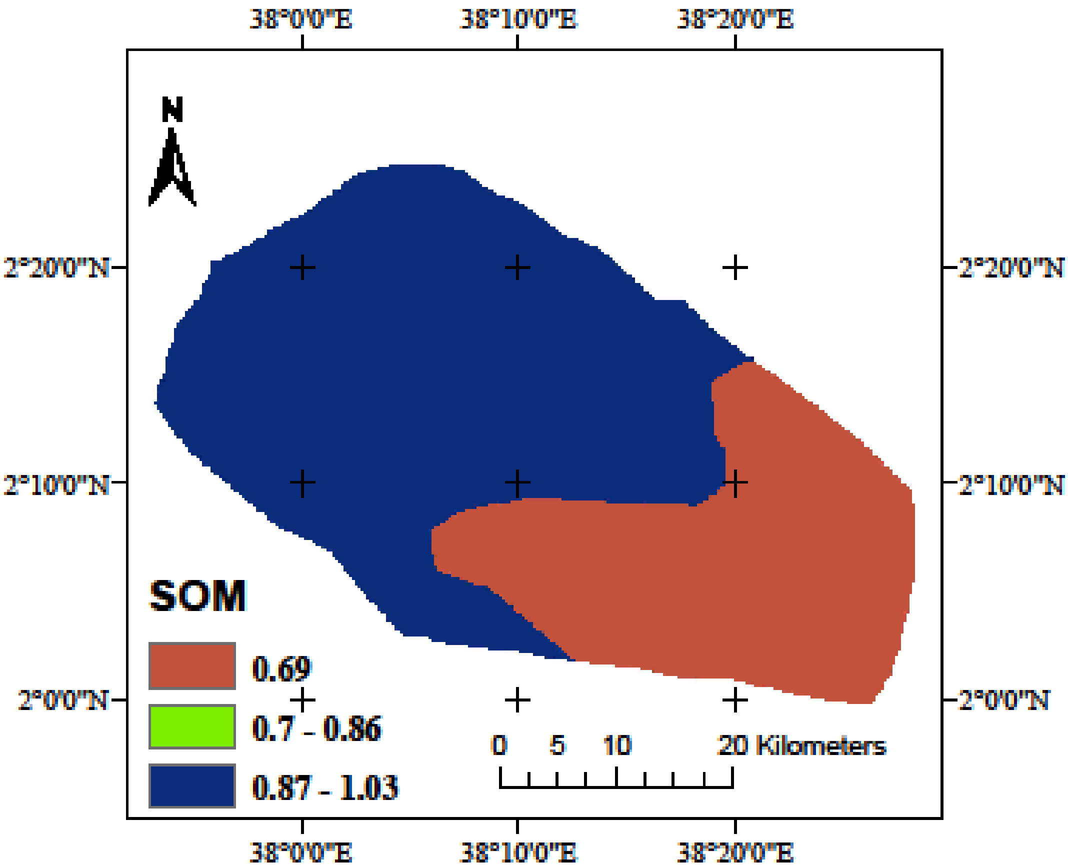

Figure A4. Soil organic matter (SOM) map

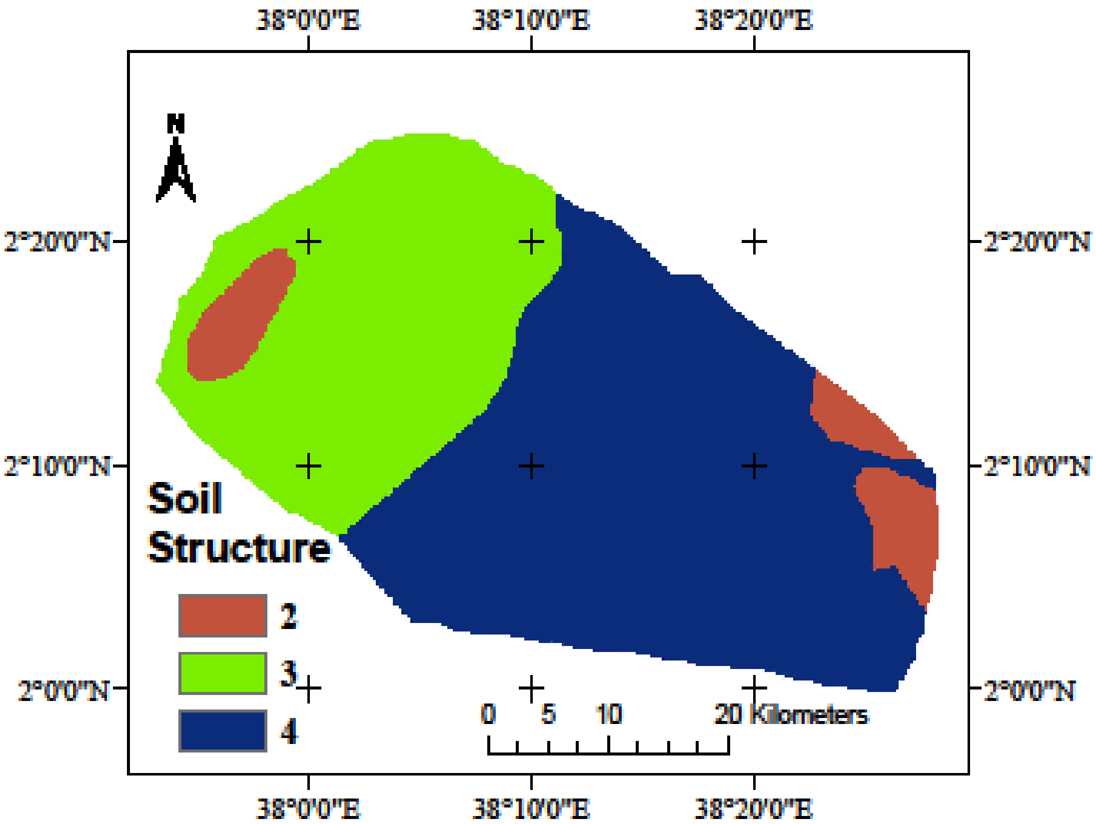

Figure A5. Soil structure code map

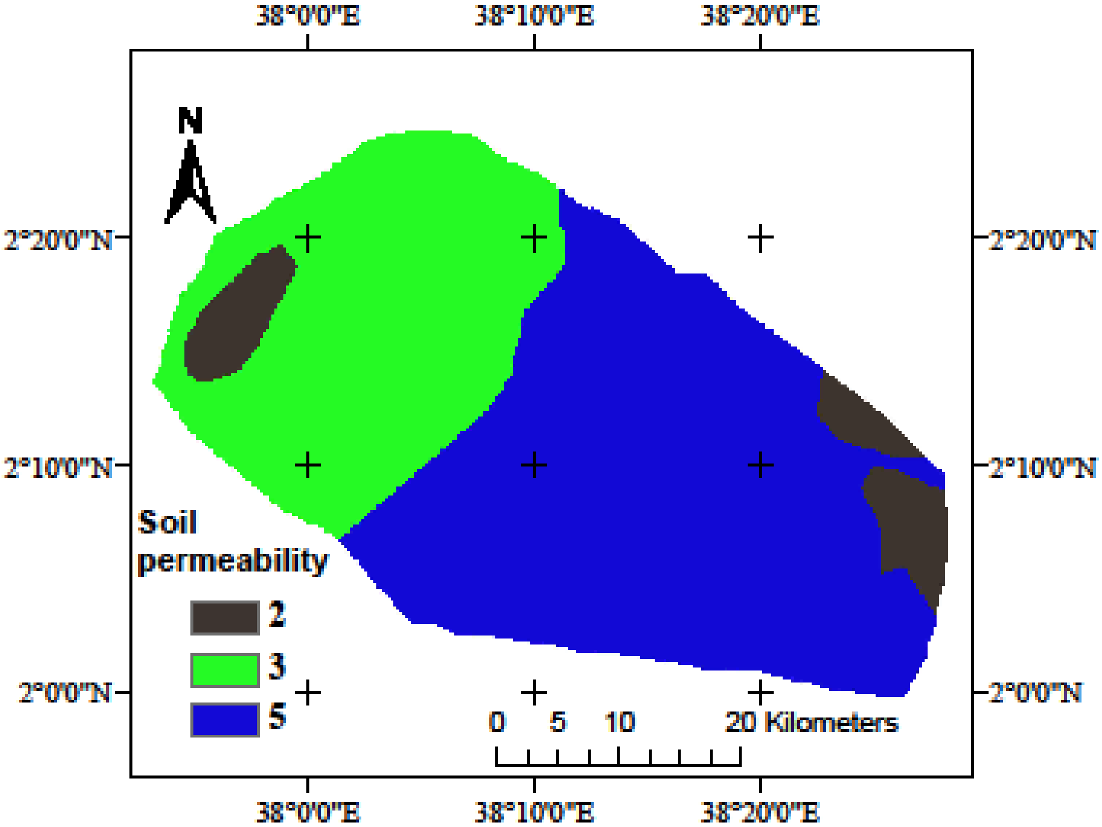

Figure A6. Soil permeability code map

Appendix III: LS factor parameters maps

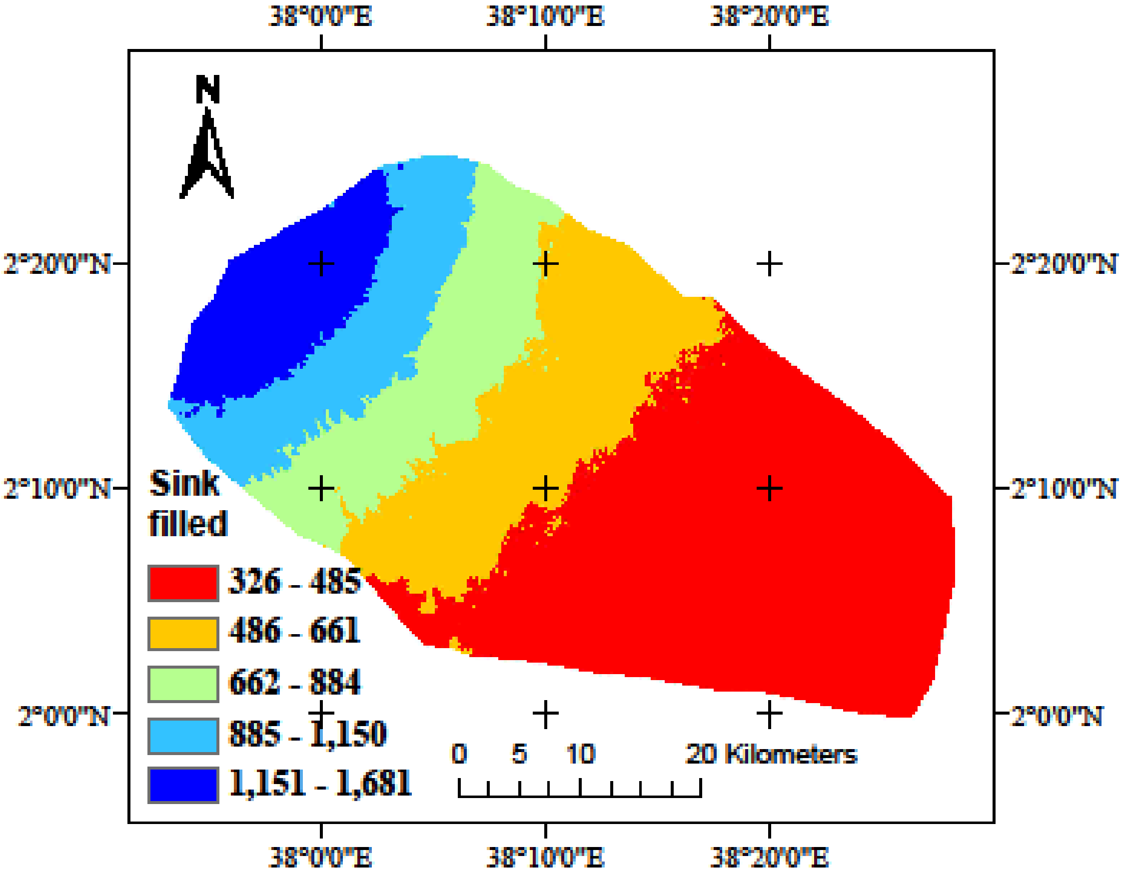

Figure A7. Sink filled map

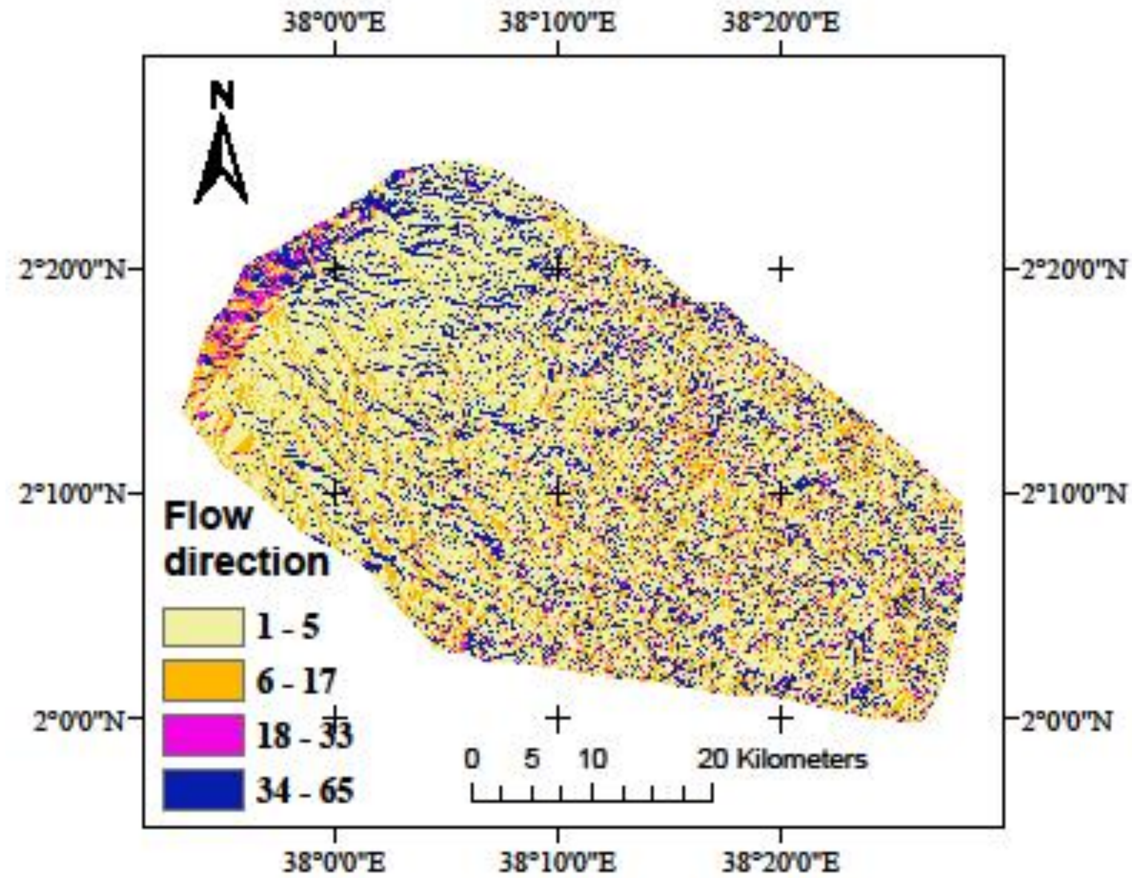

Figure A8. Flow direction map

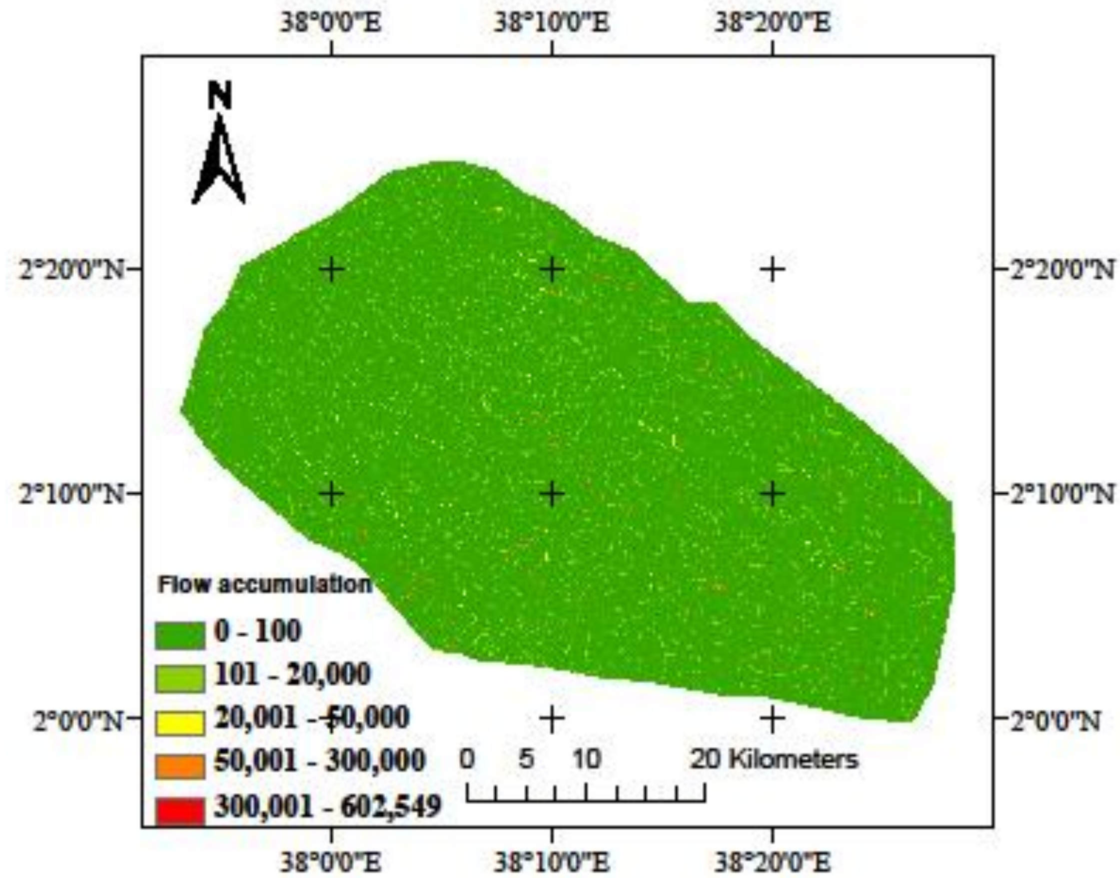

Figure A9. Flow accumulation map

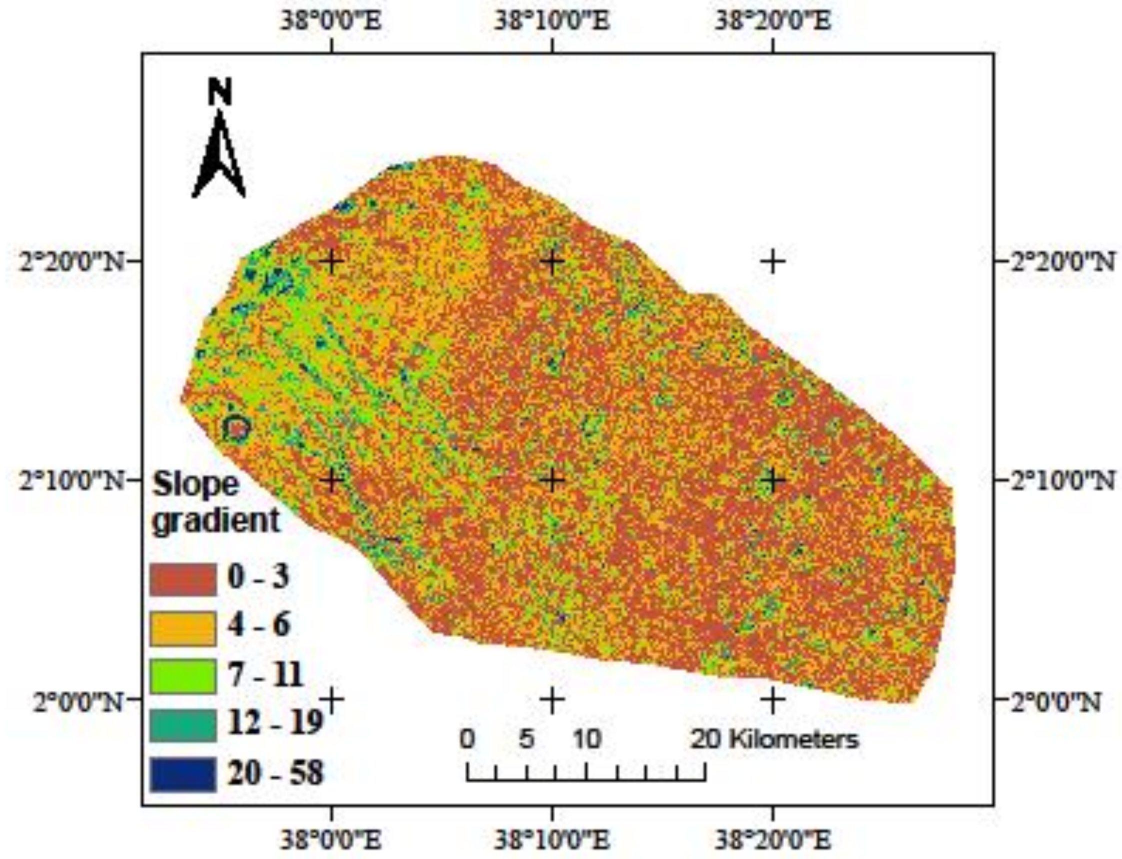

Figure A10. Slope gradient map

Appendix IV: C factor parameters maps

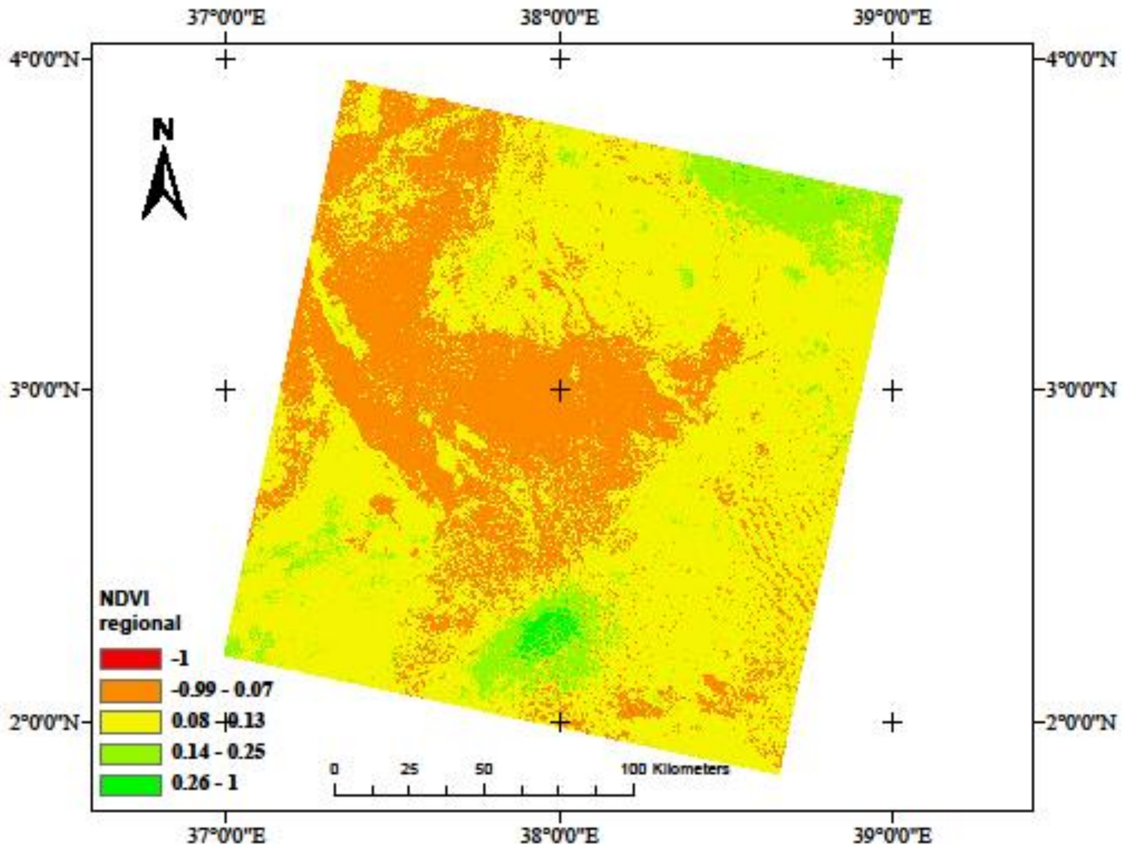

Figure A11. Regional NDVI

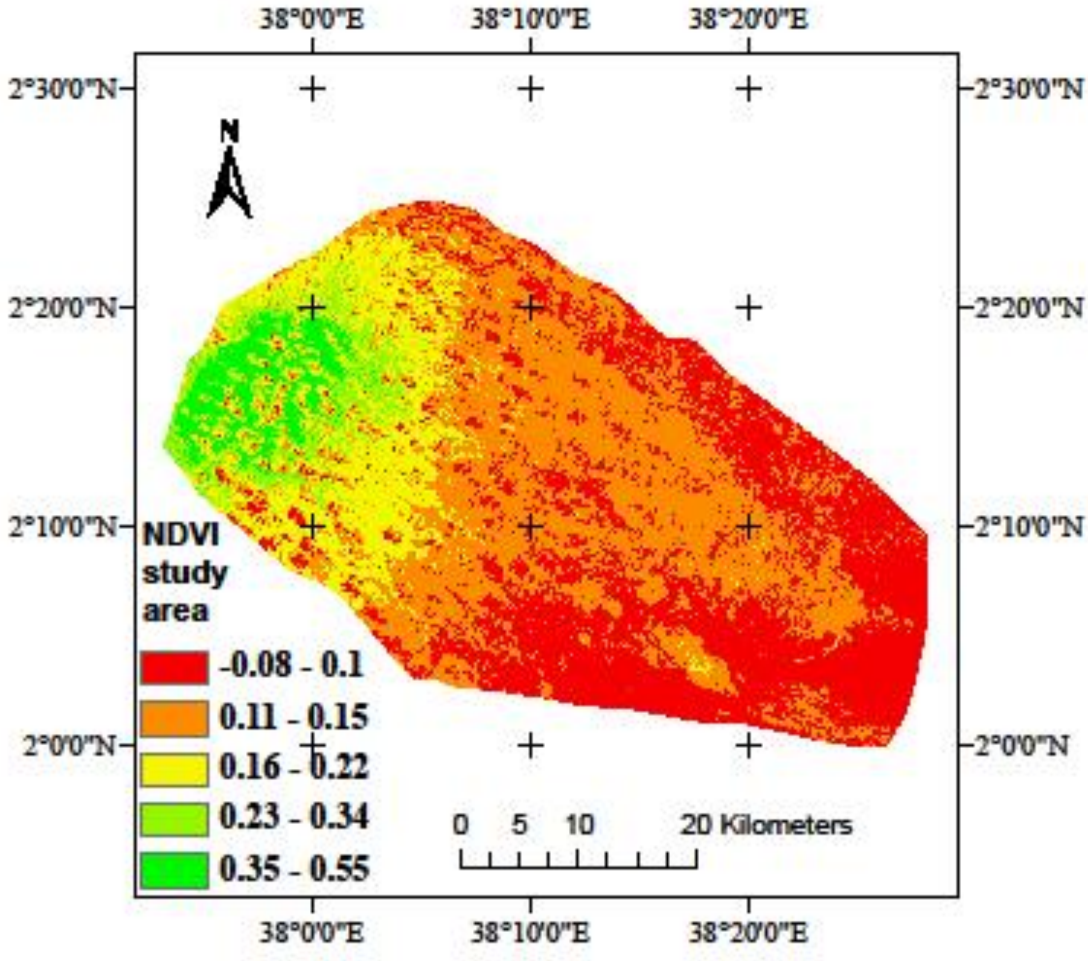

Figure A12. Study area NDVI

Appendix V: P-factor maps

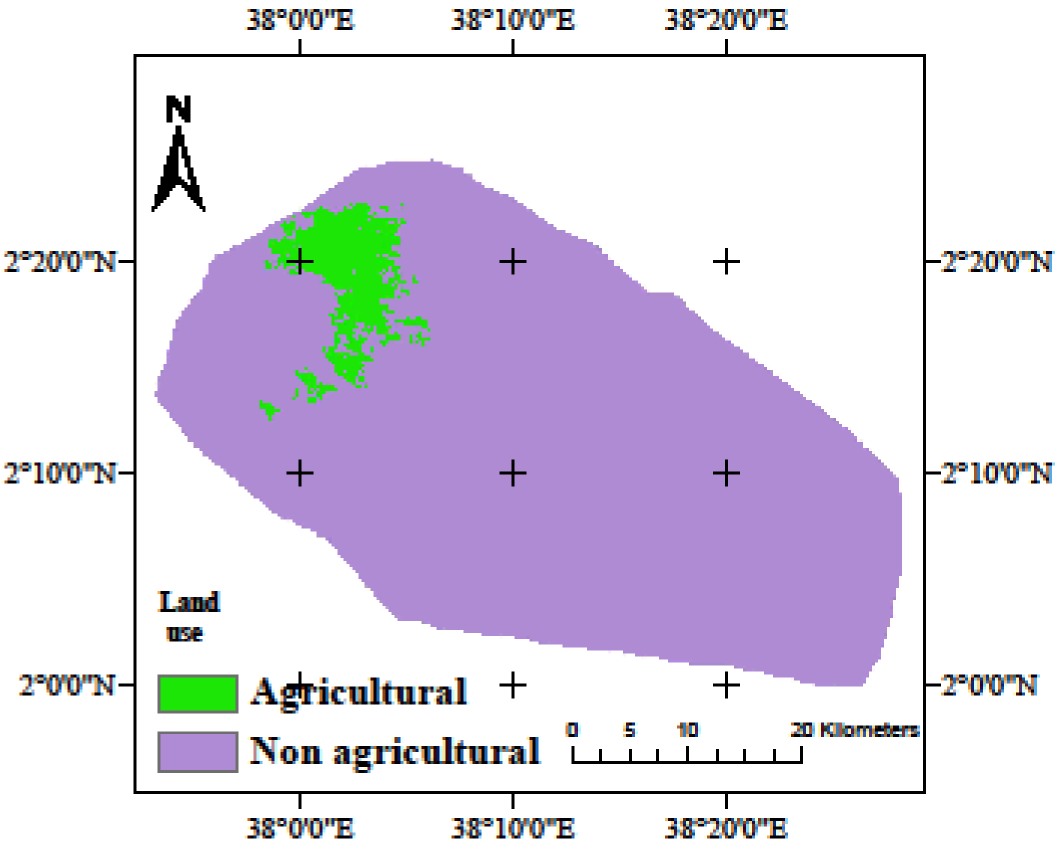

Figure A13. Land use map showing agricultural and non-agricultural areas of the study area

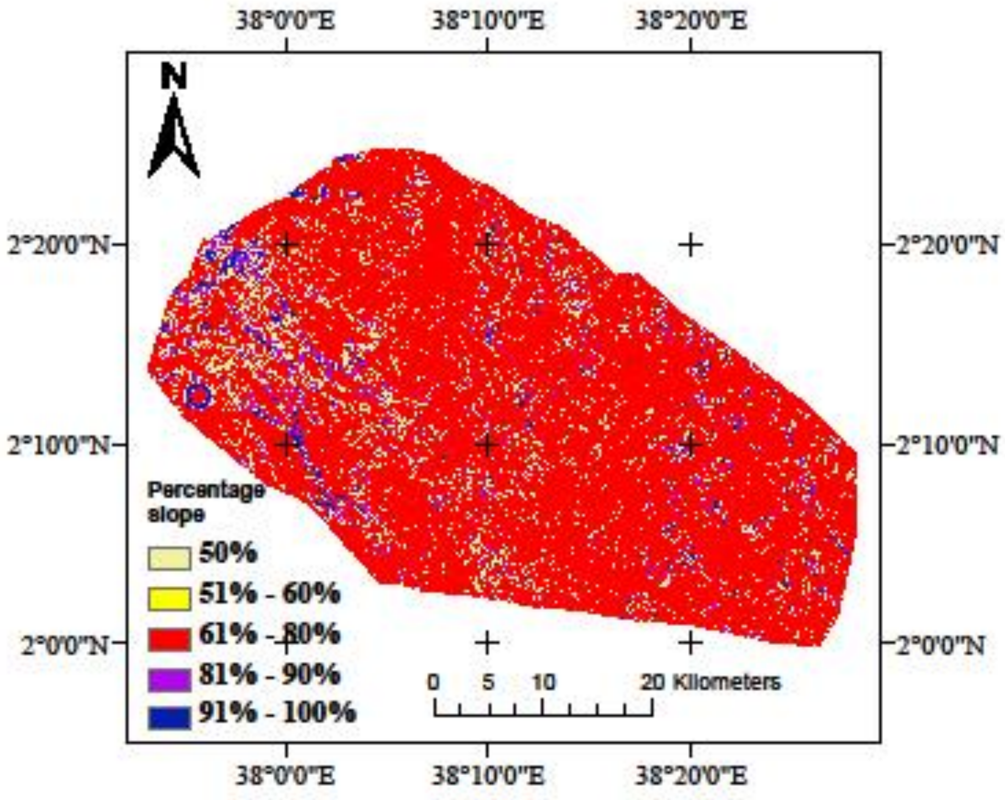

Figure A14. Reclassified slope map of the study area

Appendix VI: The major soil properties of the study area

Table A2. The major soil properties of the study area

Value	FAO soil units	CEC	Texture	Structure (ST)	Permeability (Perm)	ST code	Perm code
1	Lithosols	4	Loamy	Blocky	Moderate	3	3
2	Chromic Cambisols	4	Loamy	Aggregate	High	2	2
3	Pellic vertisols	4	Clayey	Massive	Low	4	5
4	Eutric Nitosols	3	Clay	Blocky	Moderate	3	3
5	Mollic Andosols	4	Very clayey	Aggregated	High	2	2
6	Calcic Xerosols / Yamosols	3	Clayey	Massive	Low	4	5
7	Calcic Xerosols / Yamosols	3	clayey	Massive	Low	4	5
8	Calcaric Fluvisols	7	Very clayey	Massive	Low	4	5
9	Luvo-orthic Solonetz	4	Clayey	Massive	Low	4	5

Appendix VII: Rainfall data

station ID	Station na	Elem	Year	1	2	3	4	5	6	7	8	9	10	11	12	Total
8737000	MARSABIT	Preci	1980	13	3	4	102	138	0	11	29	2	11	45	3	358
8737000	MARSABIT	Preci	1981	2	0	203	537	104	7	6	9	1	197	69	35	1170
8737000	MARSABIT	Preci	1982	3	0	13	566	286	8	7	4	1	342	130	111	1470
8737000	MARSABIT	Preci	1983	4	23	1	337	51	4	36	11	21	16	33	31	566
8737000	MARSABIT	Preci	1984	0	0	2	180	16	1	6	1	14	110	200	16	545
8737000	MARSABIT	Preci	1985	19	51	99	345	365	19	3	9	4	112	69	55	1151
8737000	MARSABIT	Preci	1986	0	0	73	225	12	8	6	0	1	34	125	35	518
8737000	MARSABIT	Preci	1987	45	0	11	169	298	37	15	16	4	2	73	15	687
8737000	MARSABIT	Preci	1988	32	3	60	512	15	11	5	9	49	121	140	58	1016
8737000	MARSABIT	Preci	1989	57	39	32	300	77	12	3	4	0	55	202	38	818
8737000	MARSABIT	Preci	1990	53	133	61	302	23	14	0	0	1	21	110	149	868
8737000	MARSABIT	Preci	1991	47	1	110	68	16	4	26	20	4	0	28	88	410
8737000	MARSABIT	Preci	1992	1	47		146	23	2	12	4	1	57	90	158	539
8737000	MARSABIT	Preci	1993	104		11	241	244	17	5	1	1	74	59	11	768
8737000	MARSABIT	Preci	1994	0	0	8	112	72	1	27	11	3	209	1	70	513
8737000	MARSABIT	Preci	1995	0	76	43	371	121	1	4	19	1	47	138	33	854
8737000	MARSABIT	Preci	1996	8	3	46	81	27	69	7	4	6	1	68	0	320
8737000	MARSABIT	Preci	1997	0	0	43	347	2	3	2	0	5	430	473	140	1444
8737000	MARSABIT	Preci	1998	277	41	110	104	191	32	14	3	0	1	111	9	893
8737000	MARSABIT	Preci	1999	1	0	27	144	9	6	5	9	2	11	92	32	337
8737000	MARSABIT	Preci	2000	8	0	1	11	1	9	1	0	8	8	40	13	100
8737000	MARSABIT	Preci	2001	33	3	70	181	11	8	7	27	0	23	193	46	603
8737000	MARSABIT	Preci	2002	19	3	120	255	53	6	13	13	5	55	42	311	895
8737000	MARSABIT	Preci	2003	0	0	18	263	64	13	0	17	7	36	220	76	713
8737000	MARSABIT	Preci	2005	1	1	0	177	248	10	1	3	1	111	20	2	572
8737000	MARSABIT	Preci	2007	8	7	16	102	77	10	25	28	12	109	83	7	482
8737000	MARSABIT	Preci	2008	77	0	22	148	7	2	3	12	3	100	289	3	666
8737000	MARSABIT	Preci	2009	11	19	7	26	10	5	0	0	0	195	35	85	391
8737000	MARSABIT	Preci	2010	45	54	77	93	36	0	16	5	2	38	22	4	391
8737000	MARSABIT	Preci	2011	0	33	0	81	5	6	1	2	0	239	477	9	853
8737000	MARSABIT	Preci	2012	0	1	1	269	51	11		11	9	157	88	135	733
8737000	MARSABIT	Preci	2013	44	3	347	303	21	2	18	7					744

station ID	Station r	Eleme	Year	1	2	3	4	5	6	7	8	9	10	11	12	Total
8639000	MOYALE	Precip	1980	1.2	2.3	35.7	54.8	204	1.4	12.2	53.1	26.2	30.3	94.2	8.1	523
8639000	MOYALE	Precip	1981	0	5.6	182	343	65.1	20.9	6.9	14.6	12	76.8	79.2	8.9	816
8639000	MOYALE	Precip	1982	2	4.5	22.7	238	470	14.5	13.6	1.7	118	213	75.8	20.9	1195
8639000	MOYALE	Precip	1983	23.7	26.8	2.4	215	178	41.6	20.7	0.4	17.2	20.1	36.1	18.9	601
8639000	MOYALE	Precip	1984	0.9	0.2	14.9	52.1	98.3	6.3	10.2	0.4	5.3	59.3	96.5	27.5	372
8639000	MOYALE	Precip	1985	37.8	27.7	150	166	282	27.9	9.1	12.1	9.4	153	19.9	4.8	900
8639000	MOYALE	Precip	1986	0	17.6	14.6	287	60.7	22.8	16.5	1	7.7	63.3	141	51.9	684
8639000	MOYALE	Precip	1987	18.1	10.1	51.4	138	273	4.6	5.2	32.4	9.3	12.1	50.2	4.7	609
8639000	MOYALE	Precip	1988	8.6	32.4	33.9	361	19.5	50	0	20.2	84.6	41.3	67.6	43.8	763
8639000	MOYALE	Precip	1989	19.4	47.6	44.6	213	157	33.9	5.1	5.7	6.8	58.2	125	94.2	811
8639000	MOYALE	Precip	1990	12.1	84.3	41.4	226	71.2	12.6	3.2	0.4	2.7	96.3	50.2	79.7	680
8639000	MOYALE	Precip	1991	30.9	47.5	58.4	71.8	184	15.5	59.8	20	0	29	26.3	13.3	557
8639000	MOYALE	Precip	1992	2.2	14.1	24.3	94.7	117	10.2	23.9	6.3	50.2	43.2	168	59	613
8639000	MOYALE	Precip	1993	42	24.5	38.2	67.2	205	37.3	9.8	0	1.4	73.4	50.5	6.3	556
8639000	MOYALE	Precip	1994	0	0	38	78.3	98.3	17.7	9.8	1.5	20.1	137	219	25.5	645
8639000	MOYALE	Precip	1995	0	35.7	121	99.2	46.9	10.1	21.9	20.4	4.6	88.5	44.9	18.5	512
8639000	MOYALE	Precip	1996	8.3	0.1	103	109	122	10.8	13.5	0.3	7.6	20.3	59.9	11.8	466
8639000	MOYALE	Precip	1997	0	0	41.7	305	21.8	21.3	7.5	3	11.3	605	277	51.1	1345
8639000	MOYALE	Precip	1998	116	67.9	16.1	238	148	56.3	18.2	21.1	1.5	9.9	59.3	23.4	776
8639000	MOYALE	Precip	1999	0.6	1.5	71.1	81.3	66.5	23.5	8	12.4	0.7	92.1	69	29.4	456
8639000	MOYALE	Precip	2000	15.9	0	0	70.9	82.1	5	11.9	21.9	20.6	72.5	53.6	27.9	382
8639000	MOYALE	Precip	2001	16.7	21.8	141	179	18.3	9.3	6.8	16.8	12.1	20	91.2	16.5	550
8639000	MOYALE	Precip	2002	5.8	0	62.9	197	83.4	15.2	3	2.5	43.5	149	27.3	107	697
8639000	MOYALE	Precip	2003	23.2	3.8	39.3	0.8	96.3	12.6	2.7	13.9	12.3	8.6	140	20.2	374
8639000	MOYALE	Precip	2005	11.4	0	10.5	60.1	149	22.1	10.2	2.6	2.1	24	47.6	0	340
8639000	MOYALE	Precip	2007	5.3	19.1	33.8	130	90.2	25.4	4.2	35.3	16	118	88.6	0.6	567
8639000	MOYALE	Precip	2008	6.2	0	87.1	150	68.9	43.2	11.4	9.8	10.6	186	53.1	3.4	629
8639000	MOYALE	Precip	2009	68.6	1.1	33.6	107	84.9	10.9	0	1.7	0.7	78.4	95	30.2	512
8639000	MOYALE	Precip	2010	8.3	34.9	62.7	260	13.6	7	14.3	3.1	3.8	82.5	2.7	0.3	493
8639000	MOYALE	Precip	2011	0.7	22.9	0.3	30.5	54.8	4.6	0.4	70.6	23.2	202	276	1.3	687
8639000	MOYALE	Precip	2012	0	19.6	24.2	97	69.2	0.8	0.1	21.3	32.7	91	113	48.5	517
8639000	MOYALE	Precip	2013	18.8	0	182	218	84.1	25	11.5	12.8	1.3				553

Appendix VIII: Thesis published article

This research findings were published in the Open Journal of Soil Science (OJSS).

Njiru, G, Kariuki, P, and Mwetu, K. (2018) Modelling Soil Erosion for Land Management in Ungauged Golole Catchment in Marsabit County, Kenya. Open Journal of Soil Science, 8, 277-302, doi.org/10.4236/ojss.2018.811021